

MINT 709, Capstone Project

High Intensity Light Emitting Diodes in an Underwater
Environment

Written by, Colin Chamberlain
June, 2006

1st Reader: Professor M. MacGregor

2nd Reader: Prof. J. Harms

Abstract

The Victoria Experimental Network Under the Sea (VENUS) project will be deployed in three location by December 2006. This network provides telecommunication and internet access to the sea floor. It will be possible to connect a sensor network to a VENUS node in order to access data measured by the sensor network. An undersea sensor network could use acoustic or optical transmission. This paper investigates the use of high intensity light emitting diodes as a transmission source for such a network. The criteria tested are energy conservation, path loss, viewing angle and minimum pulse width. The paper also provides a discussion of penetration by light in turbid coastal waters and a discussion of the potential for mutipath fading by transmitted light in sea water.

Table of Contents

1.	Introduction	4
1.1.	The Venus Project	4
1.2.	Sensor Networks and Their Weaknesses	6
2.	Optical Penetration in Turbid Saline Water	8
3.	Multipath Fading	10
4.	Performance	11
4.1.	Performance Tests	12
4.1.1.	LED Input Power versus Irradiant Output Power	13
4.1.2.	Diode Path Loss	14
4.1.3.	Diode Irradiant Output Power over a Viewing Angle.....	15
4.1.4.	Diode Minimum Pulse Width	15
4.2.	Test Results	18
4.2.1.	OVLFG3C7 [13]	18
4.2.2.	OVLGCOC6B9 [13]	20
4.2.3.	OVLFB3C7 [13]	22
4.2.4.	67-1755-ND [13].....	24
4.2.5.	67-1115-ND [13].....	26
4.2.6.	SSL-DSP5093USBC [13]	28
4.2.7.	SSL-DSP5093UPGC [13].....	30
4.2.8.	RL5-V1015 [14].....	32
4.2.9.	RL5-B4630 [14]	34
4.2.10.	RL5-B5515 [14]	36
4.2.11.	RL5-A7032 [14].....	38
4.2.12.	RL5-G7532 [14].....	40
4.2.13.	RL5-G8045 [14].....	42
4.2.14.	475-1126-1-ND [13]	44
4.2.15.	475-1198-1-ND [13]	46
4.2.16.	475-1199-1-ND [13]	48
4.2.17.	441-1089-ND [13].....	50
4.2.18.	441-1102-ND [13].....	52
4.2.19.	441-1092-ND [13].....	54
4.2.20.	441-1099-ND [13].....	56
4.3.	Performance Analysis	58
5.	Conclusions	58
6.	Recommendations	59
7.	References	59
	Appendix A. Light Emitting Diodes Investigated.....	61
	Appendix B. Circuit Designs	63

1. Introduction

Sensor networks have several applications including scientific research. Sensor networks are made up of several sensors units (sometimes referred to as motes). Each sensor must provide communications using transmission and reception, some signal processing capability and a protocol used to network the data between sensors. Historically these sensor networks provide wireless communication. Undersea sensor networks must use another form of communication. This communication may be either optical or acoustic.

1.1. The Venus Project

The Victoria Experimental Network Under the Sea (VENUS) provides a means of monitoring the ocean environment. It provides telecommunications and internet access to instruments on the ocean floor. [1] Conceived and funded in 2001, the VENUS project is intended to provide real time access to data on the sea floor.

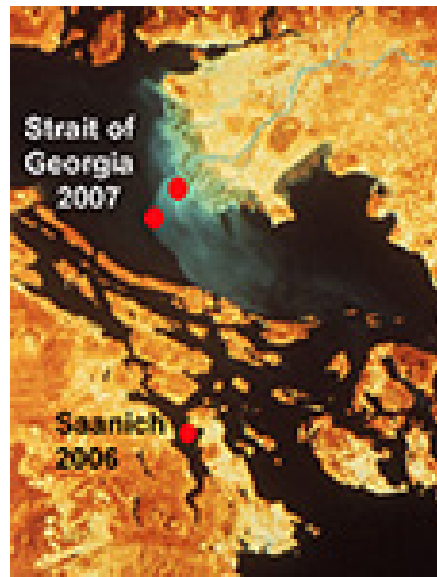


Figure 1
Locations of Project Venus Arrays [1]

By December 2006 project Venus will be deployed in three locations – the Saanich Inlet, the Strait of Georgia and the Fraser Delta, as shown in Figure 1 above. Each array has five elements: [2]

- Arrays of scientific instruments and vertical profiling instrument packages;
- Electro-optical cables on the sea floor;
- Shore station interfaces for power and two-way communication to the instruments;
- A data management, archive and distribution centre;
- An operations centre to monitor and control all subsea and shore station elements.

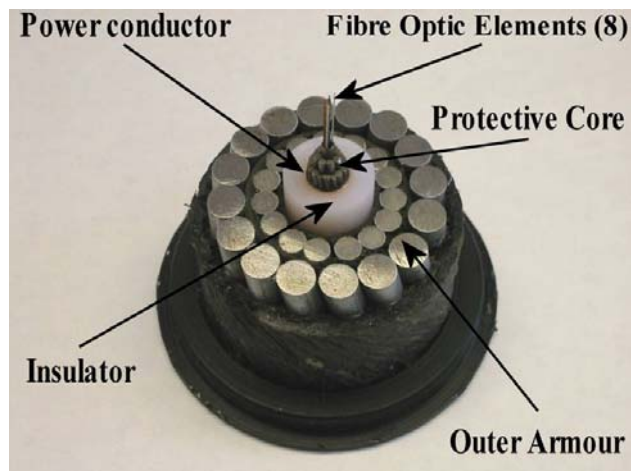


Figure 2
The Electro-Optical Cable [1]

The instruments (this could be a sensor network) are connected to a node. The node, as shown in Figure 3, in turn is interfaced to the main cable which provides power and fibre optic connectivity to the surface.



Figure 3
VENUS Node [1]

Figure 4 is a graphical representation of the VENUS System. Below the surface the instrument package is interfaced to the VENUS Node through the Scientific Instrument Interface Module (SIIM). The VENUS Node is connected to the main cable for power and to allow the flow of data to the surface. The Network operations centre then oversees the flow of data to the Data Management and Archive system and out to the internet.

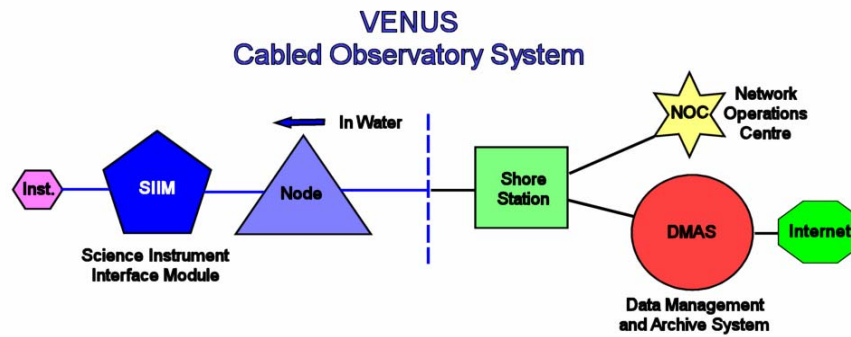


Figure 4
The Venus Architecture [1]

As previously stated, the instrument package could be an ad-hoc sensor network in which one node (not to be confused with the VENUS Node) of the network could be cabled to the VENUS Node.

1.2. Sensor Networks and Their Weaknesses

*“A **sensor network** is a computer network of many, spatially distributed devices using sensors to monitor conditions at different locations, such as temperature, sound, vibration, pressure, motion or pollutants. Usually these devices are small and inexpensive, so that they can be produced and deployed in large numbers, and so their resources in terms of energy, memory, computational speed and bandwidth are severely constrained. Each device is equipped with a radio transceiver, a small microcontroller, and an energy source, usually a battery. The devices use each other to transport data to a monitoring computer.”[3]*

The sensor network, in Figure 5 consists of a number of nodes (sometimes referred to as motes) that may be deployed from an airplane, a boat, or any number of such conveyances. The nodes in the sensor field then collect data and communicate with each other using an appropriate protocol. The network is infrastructureless and uses multiple hops to route the data through the sink to the task manager. When deployed in conjunction with the VENUS project this would be achieved through the VENUS Node.

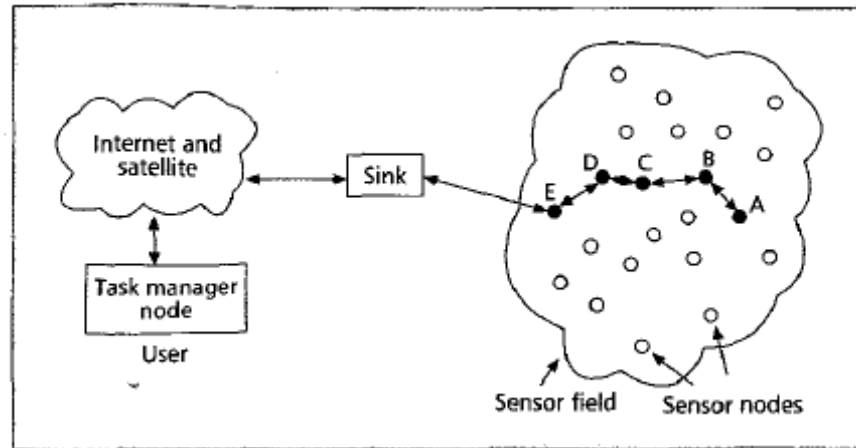


Figure 5
A Sensor Network.[4]

The failure of a single node should not result in the failure of the sensor network. The network should adapt by rerouting the data through other sensor nodes, often requiring more hops.

A sensor node is a Single Board Computer (SBC) that must include:

- Processing and data storage;
- Data sensing capability, and perhaps analog-to-digital conversion (ADC);
- A transceiver;
- An on board power source; [4]

Figure 6 is a block diagram depiction of a sensor network node.

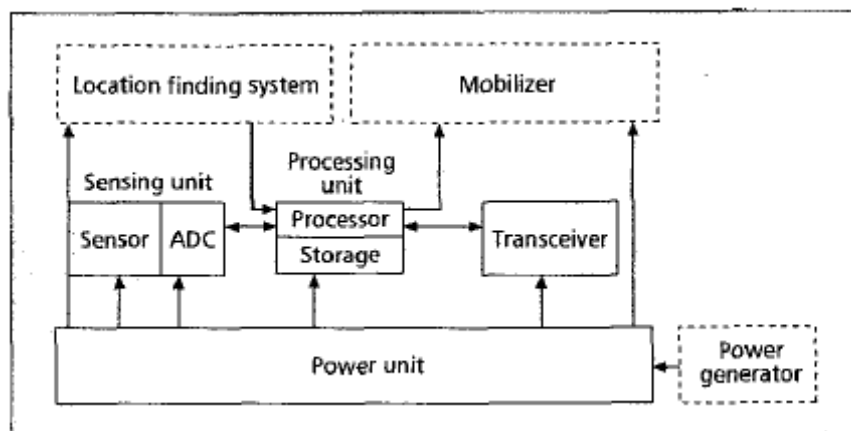


Figure 6
Block diagram of a sensor network node. [4]

The processing and data storage function contains the communications protocol used for the scattered network. A second processor, often a microcontroller, may be used to process some of the data prior to transmission.

The data sensing function is the scientific package. It is used to gather the required observed data. As discussed previously a microcontroller may contain all of the functionality needed for this task.

The transceiver is used to communicate with other nodes in the network. Typically sensor networks make use of Radio Frequency (RF) communications; however, this project will focus on optical communications beneath the water.

The power source must be small and as a result will have a limited life span. It is the power source that is the most critical point of failure. Once the sensor nodes have been deployed it is not practical to replace the power source (usually a battery) when failure occurs. When the power source in a node fails the node is lost to the network. Power consumption may be reduced by using low power components and by choosing power-aware protocols and algorithms. Power is consumed by the data sensing devices, the processor and communications [4]. This project will focus on communications.

2. Optical Penetration in Turbid Saline Water

Many factors, including particulate matter, composition, salinity, temperature, and others, affect the transmission of light through water. The attenuation coefficient $K(\lambda)$ is a measure of the light loss as a result of the combined effects of absorption and scattering [5]. The attenuation coefficient is measured in units of m^{-1} (or cm^{-1}). This coefficient is a function of the wavelength (λ) of the light being transmitted. *“The coefficient K depends mainly on the absorption of light in water and to a lesser extent on scattering.”*[6]

A simple observation of the colour of the ocean at various locations around the world leads one to the sense that visible light in the violet ($380\text{ nm} < \lambda < 455\text{ nm}$), blue ($455\text{ nm} < \lambda < 492\text{ nm}$) and green ($492\text{ nm} < \lambda < 577\text{ nm}$) spectrum will make the best penetration.

Absorption occurs when radiant energy is converted to some other form of energy, such as heat or chemical energy. Scattering occurs when the direction of the photon transport is changed without changing the wavelength. [5].

Several studies have been undertaken to determine the irradiant energy of light as it penetrates downward into seawater. This may be calculated as [7]:

$$E_0(z) = E_0(0)e^{-Kz} \quad (1)$$

$E_0(z)$ is the irradiance at depth z .

z is the depth in the water.

$E_0(0)$ is the irradiance at the surface

K is the attenuation coefficient.

The attenuation coefficient may be calculated using [8]:

$$K(\lambda) = \frac{-\ln\{E_d(\lambda, z_1)/E_d(\lambda, z_2)\}}{z_2 - z_1} \tag{2}$$

$K(\lambda)$ is the attenuation coefficient at wavelength λ .

$E_d(\lambda, z)$ is the downward irradiance at wavelength λ and depth z .

The attenuation coefficient will vary depending on water conditions. Turbid coastal waters are much different than clear ocean water. In Figure 7, values of attenuation coefficients may be estimated. For example, given a wavelength of 490 nm, the attenuation coefficient in clear ocean water is approximately 0.02 m^{-1} , while in turbid coastal water at the same wavelength the attenuation coefficient is approximately 0.65.

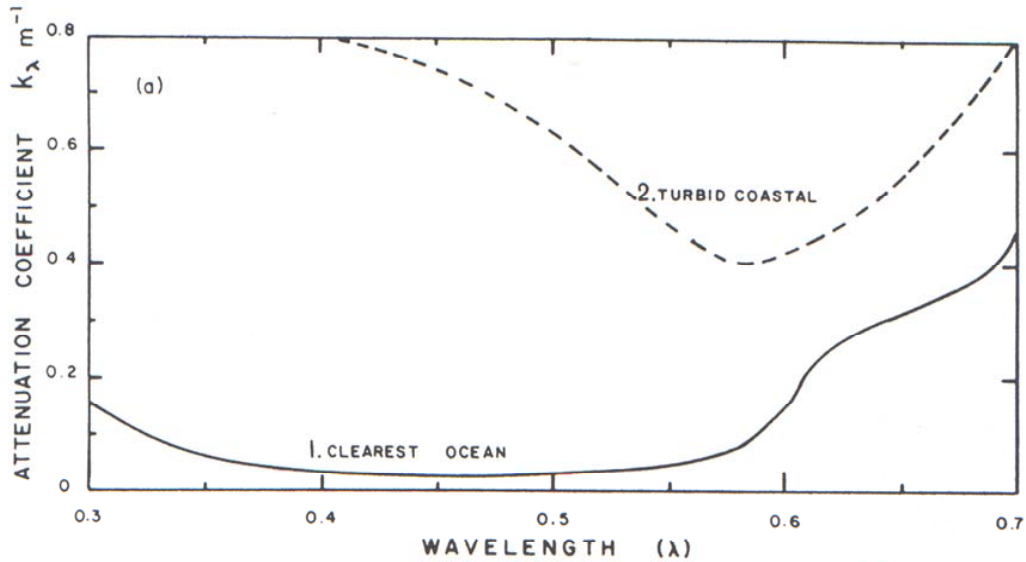


Figure 7

Attenuation Coefficient $K(\lambda)$ as a Function of wavelength (λ) in Clear Ocean Water and in Turbid Coastal Water [6]

There is a correlation between $K(490)$ and $K(\lambda)$, i.e., the attenuation coefficient at 490 nm and the attenuation coefficient at other wavelengths. These attenuation coefficients may be calculated using [8]:

$$K(412) = 1.441K(490) + 0.022 \quad \gamma^2 = 0.991 \tag{3}$$

$$K(443) = 1.364K(490) + .0007 \quad \gamma^2 = 0.997 \tag{4}$$

$$K(510) = 0.897K(490) + 0.011 \quad \gamma^2 = 0.999 \tag{5}$$

$$K(555) = 0.629K(490) + 0.046 \quad \gamma^2 = 0.985 \tag{6}$$

$$K(665) = 0.627K(490) + 0.404 \quad \gamma^2 = 0.956 \tag{7}$$

The best correlation in the above calculations occurs for $\lambda = 510$ nm, while for $\lambda = 665$ nm the poorest correlation is indicated.

Based on the previous estimate of $K(490) = 0.65 \text{ m}^{-1}$ and applying equations (1) to (7), Table 1 is a summary of attenuation coefficients and percent irradiance from the initial transmission location at distances of 0.01m, 0.05m, 0.1 m, 0.5m, 1m, 5m and 10m.

Table1 Attenuation coefficients and percent irradiance from the initial transmission location at distances indicated.

Wavelength (nm)	Attenuation Coefficient (m^{-1})	Percent Irradiance at distances shown						
		0.01m	0.05m	0.1m	0.5m	1m	5m	10m
412	0.95865	99.05	95.32	90.86	61.92	38.34	0.83	0.007
443	0.8873	99.12	95.66	91.51	64.17	41.18	1.18	0.014
409	0.65	99.35	96.80	93.71	72.25	52.20	3.88	0.15
510	0.59405	99.41	97.07	94.23	74.30	55.21	5.13	0.26
555	0.45485	99.55	97.75	95.55	79.66	63.45	10.29	1.06
665	0.81155	99.19	96.02	92.21	66.64	44.41	1.73	0.03

3. Multipath Fading

Is multipath fading a potential consideration for an optical undersea sensor network? Before addressing this question, a review of the concept of multipath fading is in order.

Multipath fading is a problem encountered in mobile communication environments. The phenomenon of multipath propagation results from signals following different paths from a transmitter to a receiver. Signals may follow a line of sight path (LOS), or they may follow a path resulting from reflection, or from diffraction or due to scattering.

Reflection occurs when a signal encounters an object that is large compared to its wavelength. In mobile radio applications this could be a large object such as the side of a building. Reflected waves undergo a 180° phase shift.

Diffraction occurs in mobile communication when a signal encounters an edge of a large object. The signal will then propagate in a different direction. A positive effect of diffraction is that a signal can be successfully sent from a transmitter to a receiver even if there is no line of sight path.

Scattering occurs when an object that is in the order of a wavelength of the signal is encountered. The result is that the signal may be scattered into several smaller signal following different paths.

The negative impact of multipath propagation is that the received signal may be affected by the simultaneous arrival of signals that may have followed different paths. Two signals arriving, one as a result of a reflected path and the other following a line of sight may destructively interfere with each other as the reflected wave undergoes a 180° phase shift. Also, due to the differing propagation times for multiple paths, signal may overlap causing intersymbol interference (ISI). ISI may effect both the amplitude of the received and combined pulse, as well as the pulse width of that received pulse.

“When a signal leaves the transmitting antenna, it gets reflected, scattered, diffracted, or refracted by various structures in its path.”[10] The presence of these obstacles may result in signal loss or fluctuation. If the signal loss is deterministic in nature and becomes random in time and space then it may be described in terms of fading. [10] *“Fading may described in terms of the primary cause (multipath or Doppler), the statistical distribution of the received envelop (Rayleigh, Rician or lognormal), the duration of fading (long-term or short term), or fast versus slow fading.”*[10]

“In free-space optical communications links, atmospheric turbulence causes fluctuations in both the intensity and the phase of the received light signal impairing link performance. The turbulence induced fading impairs free-space optical links in much the same way that flat multipath fading impairs radio-frequency wireless links.”[11] Inhomogeneities in the temperature and and pressure of the atmosphere lead to variations in the refractive index along the transmission path.

It is reasonable to assume that the sea bottom is not uniformly flat. In addition there is sea life (including reefs). These obstructions could easily present reflection and diffraction to the signal path within an optical sensor network. In addition, variations in temperature and turbulence within the water may result in similar effects to the observed free-space atmospheric turbulence effects that have been previously discussed. In addition, the turbidity of the sea water will likely result in scattering of the optical signal.

Diffraction of light can be caused by acoustic waves. This was first predicted by Brillouin in 1921. [12] Acoustic waves are accompanied by waves of refractive index variations. Light passing through these waves will be diffracted. Again, this could result in a similar effect to fading.

4. Performance

In order for an optical undersea network to be viable, the transmitting devices (Light Emitting Diodes) must be able to operate in the presented environment. The criteria for these diodes are:

- The electrical power needed to power each sensor unit is limited, and once depleted cannot practically be replaced. As a result, the power used by the light emitting diode must be kept as small as possible.
- It is not possible to predict the locations of each sensor unit in the network. Therefore, it is not possible to accurately aim the diodes at the detectors in other sensor units. To overcome this problem the viewing angle from the lens of the diode must be as wide as possible.
- The range of transmission will dictate how scattered the network can be. The irradiance of each diode must be as high as possible in order to keep the range as large as possible.
- The data transmitted by each sensor unit will be digitally encrypted (ie., pulses). It is important to understand the minimum pulse width available from each diode.

4.1. Performance Tests

The equipment used for performance testing is shown in Figure 8.



Figure 8

Test Equipment for Performance Testing of the Light Emitting Diodes

Key to the measurement is the Newport Model 841-P-USP virtual optical power meter. This, in conjunction with the 818 photodetector was used for irradiance (optical power) measurements. The default wavelength for the meter is 960 nm, however the desired wavelength may be chosen as a menu setting. This selection provides a correction factor to the power meter software. The 841-P-USP power meter together with the 818 photodetector is shown in Figure 9.



Figure 9
Newport Model 841-P-USP Virtual Power Meter and Model 818 Photodetector

4.1.1. LED Input Power versus Irradiant Output Power

In order to determine the lowest input power needed to illuminate the diodes, the irradiance of the diodes were measured as the current through the diodes was reduced. The results were plotted both as Output Power (Irradiance) versus Diode Current and as dB (using the output power at maximum current as a reference) versus Diode Current. Included in the plot was Diode Voltage versus Diode Current, and the “Dropout Current” (the current level at which the diode is no longer conducting sufficient current to illuminate). An example of the plots is shown in Figure 10(a). Three maximum diode currents were used as per the specifications of the diodes. These were 20 mA, 120 mA and 350 mA. Figure 10(b) shows the schematic diagram of the circuit used to obtain these results. Note that the value of R was 1 k Ω for 20 mA maximum current, 11 Ω for a maximum current of 120 mA and 3.9 Ω for a maximum current of 350 mA.

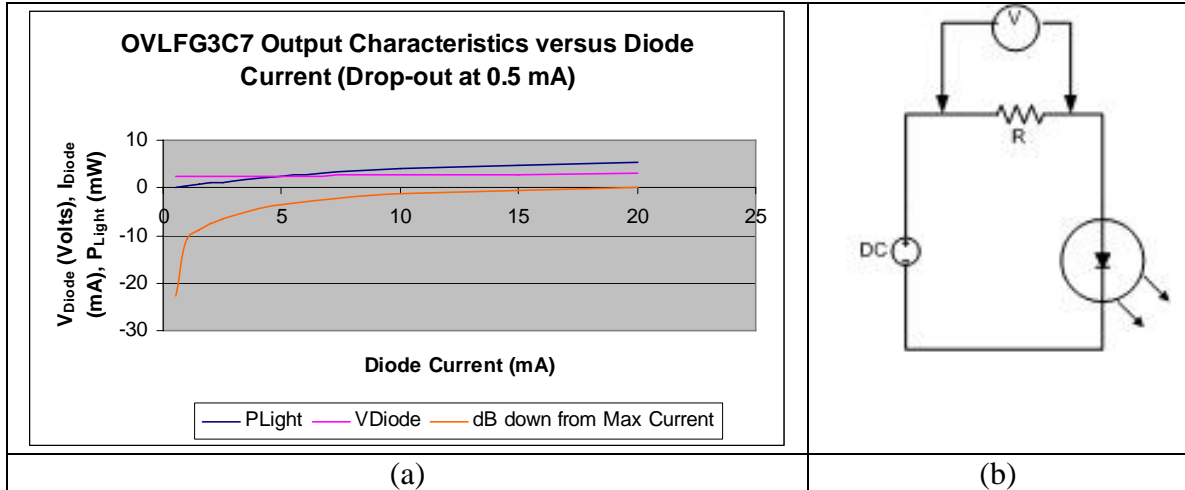


Figure 10
 (a) Example of Diode Irradiance versus Diode Current Graph, (b) Schematic Diagram of the Circuit used to obtain the Diode Irradiance versus Diode Current Data

4.1.2. Diode Path Loss

The determination of path loss for each diode was achieved by setting the diode current to a maximum value and measuring the irradiance at distances from the diode. The result was plotted in two forms; Output Power versus Distance and dB (using the output power directly in front of the diode lens as a reference) versus Distance. The circuits used to perform these measurements are the same as those shown in Figure 10(b). Examples of these graphs are shown in Figure 11(a) and 11(b).

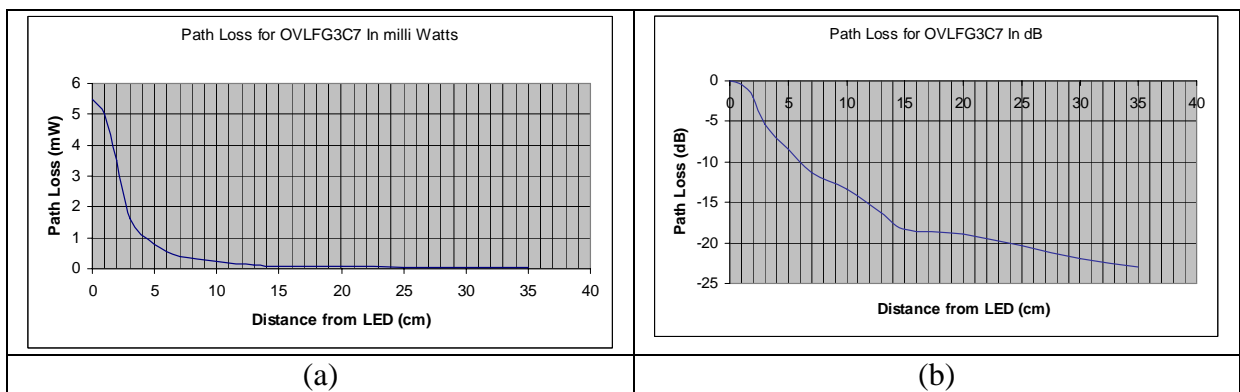


Figure 11
 (a) Example of Diode Irradiance (in Watts) versus Distance from the Diode, (b) Example of Diode Irradiance (measured in dB referenced to irradiant power at the lens of the diode) versus Distance from the Lens of the Diode

4.1.3. Diode Irradiant Output Power over a Viewing Angle

Using the data gathered in the path loss measurements, a distance from the diodes was chosen so that the irradiant power was large enough to have minimal interference from ambient light conditions. For each diode the irradiant power was measured, then at progressively larger angles from the lens the distance from the lens was measured where the same power level was achieved. The same circuit as that shown in Figure 10(a) was used for these measurements. The result was then graphed as a polar graph to show the transmission lobe. Figure 12 shows an example of the graph resulting from these measurements. The wider the lobe, the greater the viewing angle for each diode.

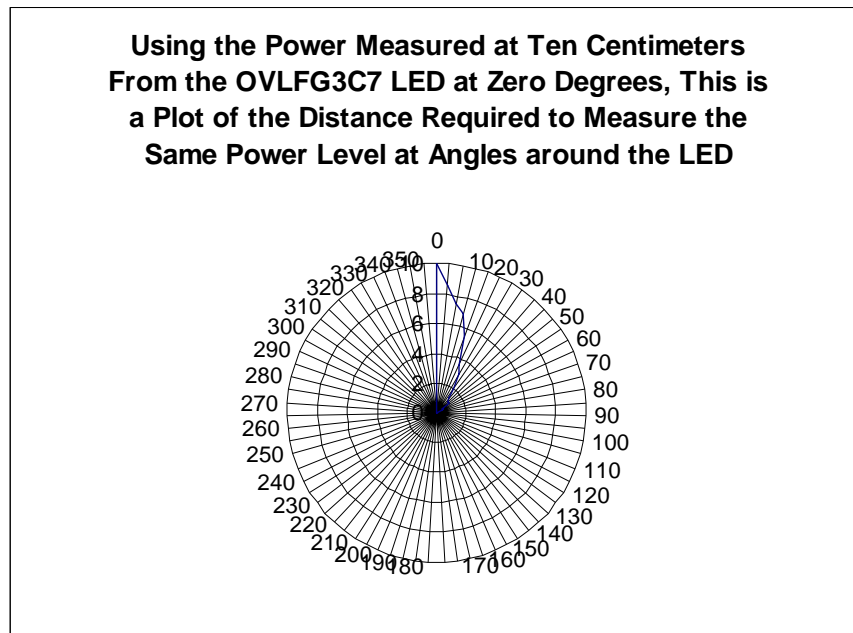


Figure 12

Example of a Graph Showing Distance from the Diode at Increasing Angles in Order to Measure a Constant Value of Irradiant Power

4.1.4. Diode Minimum Pulse Width

Measurement of minimum pulse width for the Light Emitting Diodes was accomplished using the circuits shown in Figure 13. For low current LED's the circuit in Figure 13(a) was used. For higher currents a transistor was used, as shown in Figure 13 (b), as a driver in order to avoid loading of the function generator with an internal impedance was 50 Ohms. The input pulse and resulting pulse across the diodes was measured using a Tektronix model TDS210 Oscilloscope. This Oscilloscope has a USB interface to the computer. The computer was loaded with Wavestar for Oscilloscopes software which allowed for the capture of the waveforms.

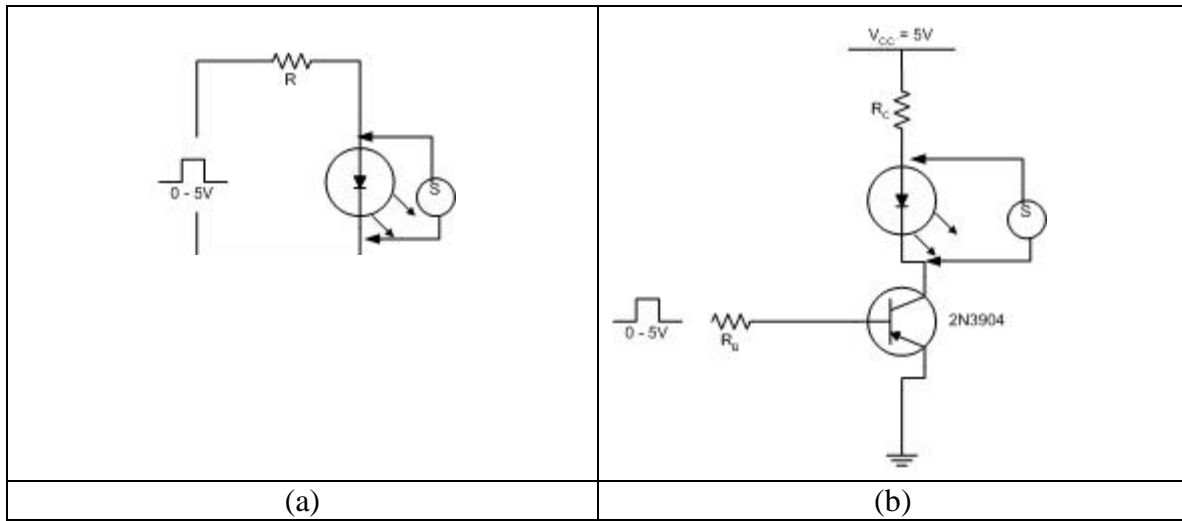


Figure 13

(a) Schematic Diagram of the Circuit used for Minimum Pulse Width Measurements for Low Current Diodes, (b) Schematic Diagram of the Circuit used for Minimum Pulse Width Measurements for High Current Diodes

Figure 14 shows an example of the captured input pulse (a) and the resulting output pulse (b). In addition the Wavestar software allows for the capture, in tabular form, of the details about any measurement. This was used for further data about the diode waveform. Figure 15 is an example of this table which is associated with the waveform shown in Figure 14 (b).

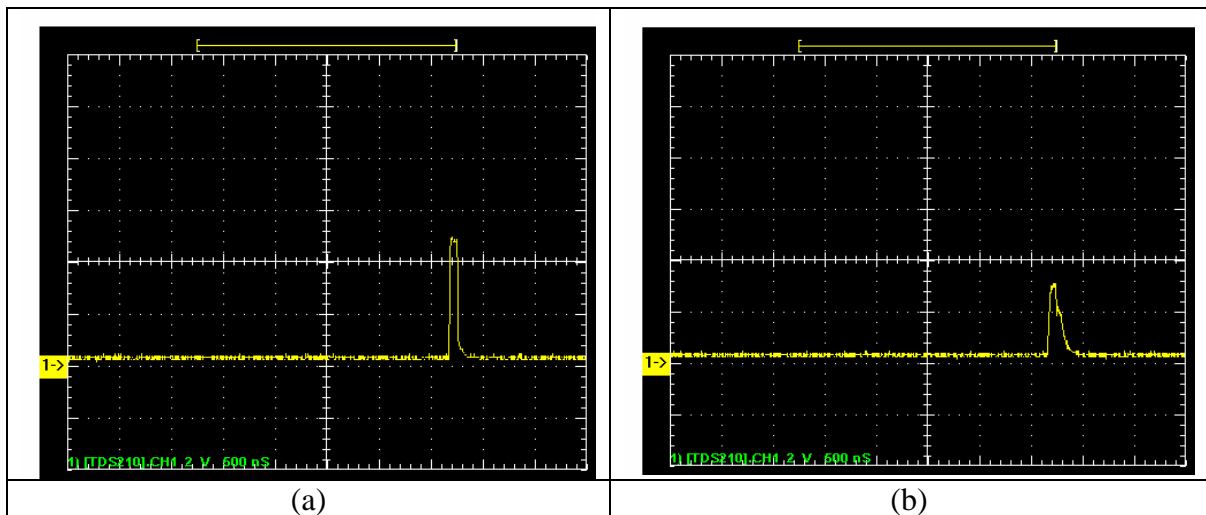


Figure 14

(a) Example of an Input Pulse to a Diode Circuit, (b) Example of a Diode Pulse

S210].Data.Waveforms.C		
Measurement Method	Automatic	
Measurement	Value	Units
Frequency	N/A	N/A
Pos. Pulse Width	124.67n	S
Neg. Pulse Width	N/A	N/A
Rise Time	28.133n	S
Fall Time	154.60n	S
Pos. Duty Cycle	N/A	N/A
Neg. Duty Cycle	N/A	N/A
Pos. Overshoot	0.0000	%
Neg. Overshoot	0.0000	%
Peak to Peak	2.9600	V
Amplitude	2.9600	V
High	3.0400	V
Low	80.000m	V
Maximum	3.0400	V
Minimum	80.000m	V
Mean	311.29m	V
Cycle Mean	N/A	N/A
RMS	473.43m	V
BurstWidth	124.67n	S
Period	N/A	N/A
Energy	1.1202u	
CEnergy	N/A	N/A
ACRMS	356.64m	V
CRMS	N/A	N/A

Figure 15
Details About the Waveform Shown in Figure 14(b)

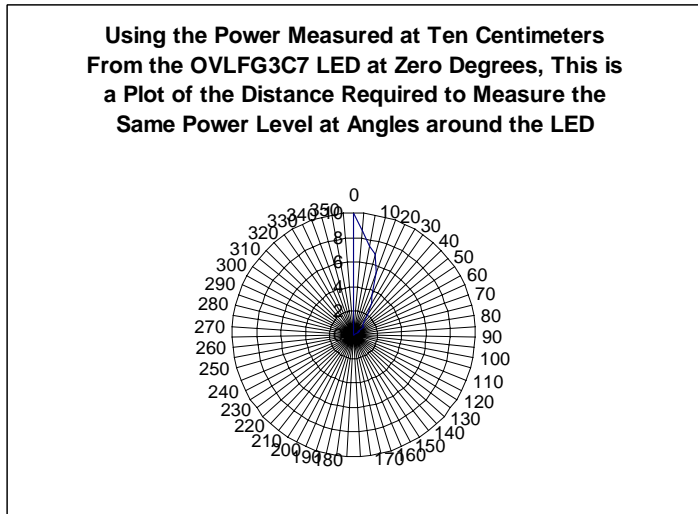
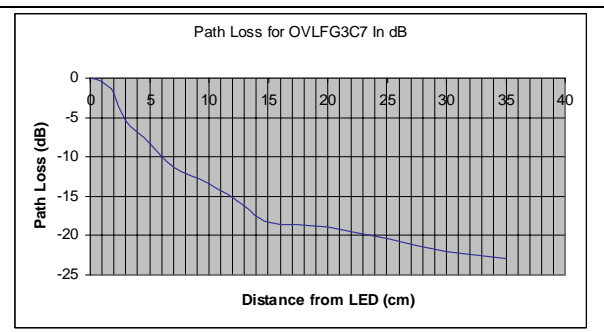
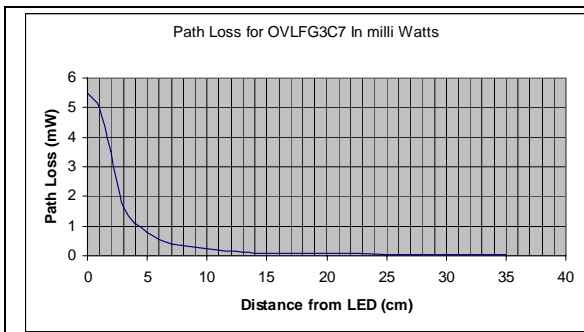
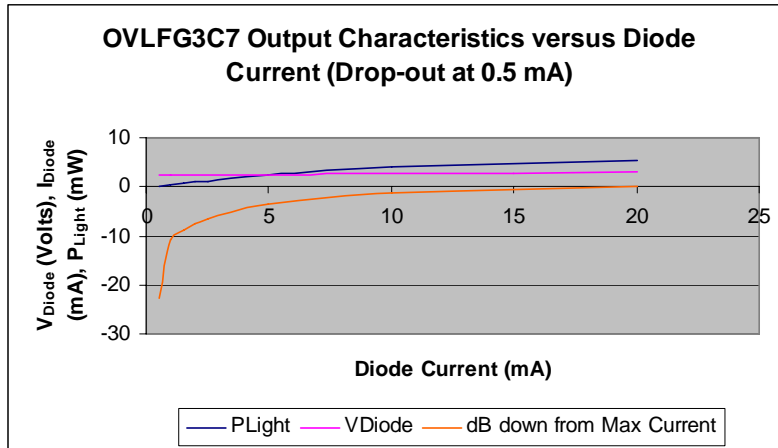
The pulse width was reduced and the irradiant power monitored just before drop-out occurred. The pulse width and irradiant power was then recorded.

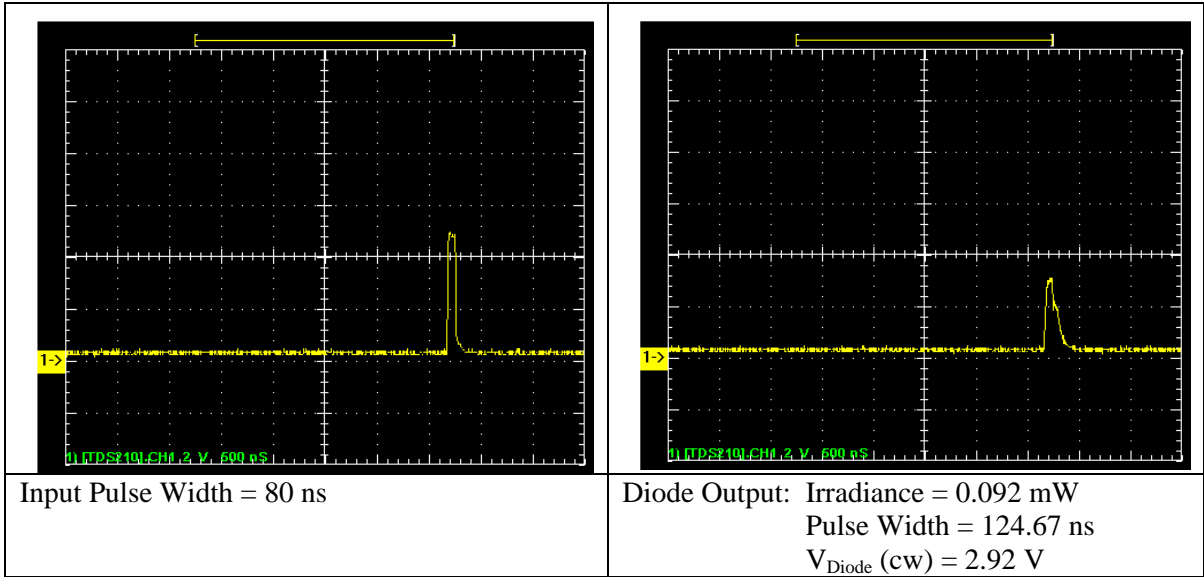
4.2. Test Results

4.2.1. OVLF3C7 [13]

Specifications

Colour	Wavelength (nm)	Luminous Intensity (Typ.) mcd @ If(mA)	Viewing Angle (X2 Theta)
Green	525	5200 20	30 degrees



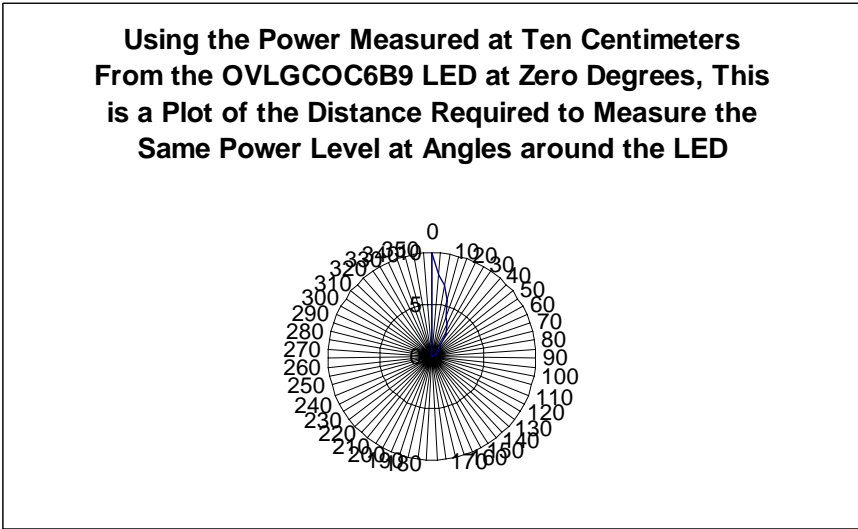
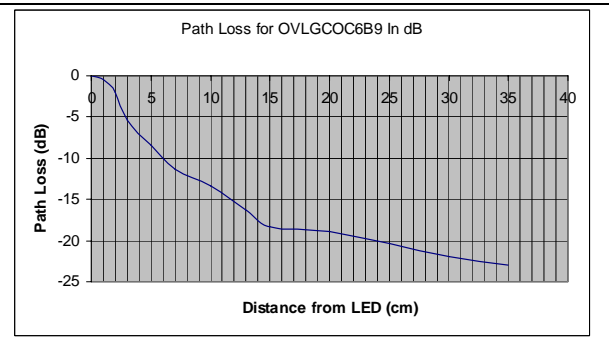
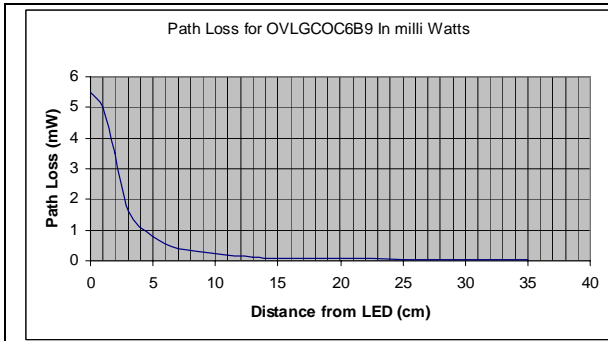
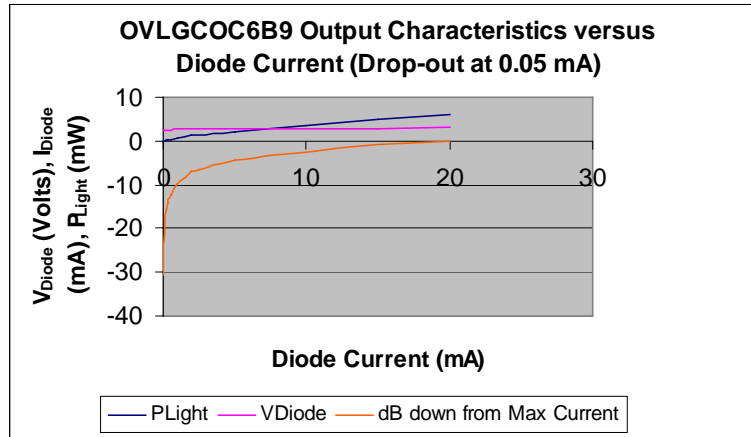


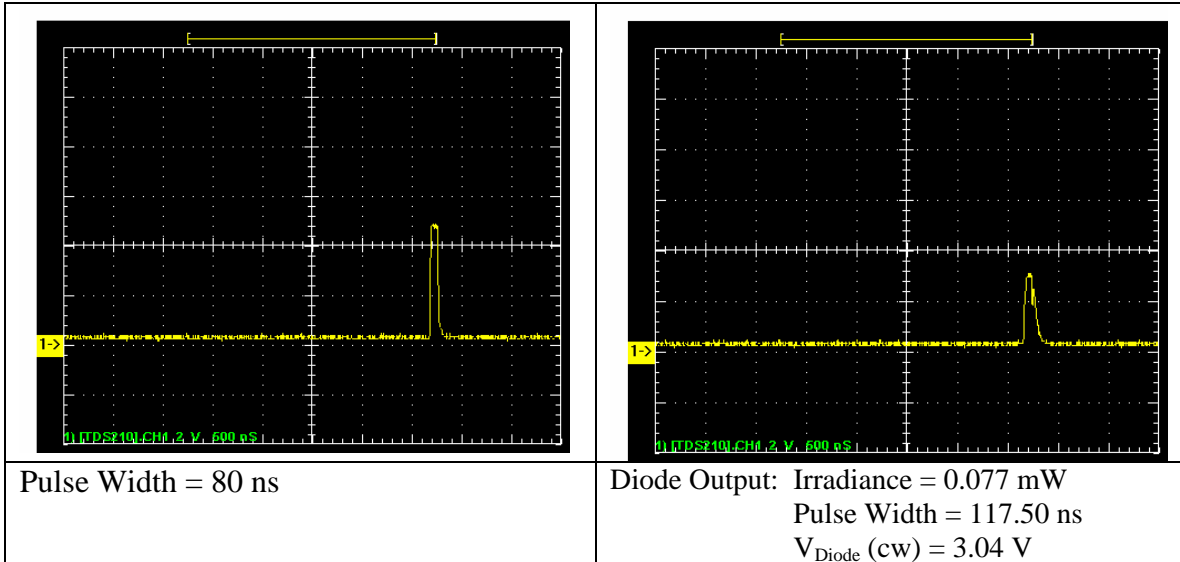
S210].Data.Waveforms.C		
Measurement Method	Automatic	
Measurement	Value	Units
Frequency	N/A	N/A
Pos. Pulse Width	124.67n	S
Neg. Pulse Width	N/A	N/A
Rise Time	28.133n	S
Fall Time	154.60n	S
Pos. Duty Cycle	N/A	N/A
Neg. Duty Cycle	N/A	N/A
Pos. Overshoot	0.0000	%
Neg. Overshoot	0.0000	%
Peak to Peak	2.9600	V
Amplitude	2.9600	V
High	3.0400	V
Low	80.000m	V
Maximum	3.0400	V
Minimum	80.000m	V
Mean	311.29m	V
Cycle Mean	N/A	N/A
RMS	473.43m	V
BurstWidth	124.67n	S
Period	N/A	N/A
Energy	1.1202u	
CEnergy	N/A	N/A
ACRMS	356.64m	V
CRMS	N/A	N/A

4.2.2. OVLGCOC6B9 [13]

Specifications

Colour	Wavelength (nm)	Luminous Intensity (Typ.) mcd @ If(mA)	Viewing Angle (X2 Theta)
Blue-Green	505	8000 20	6 degrees



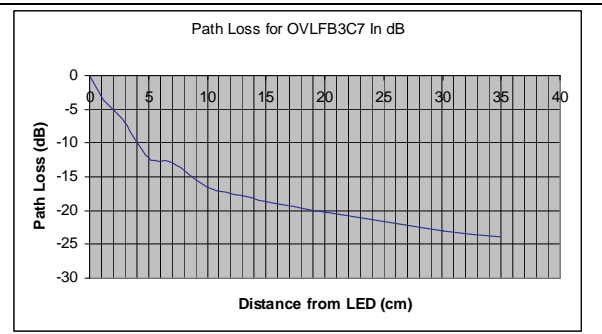
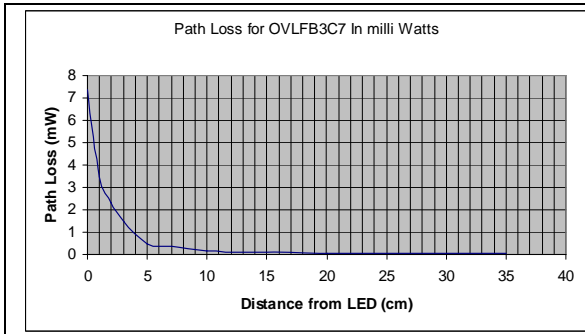
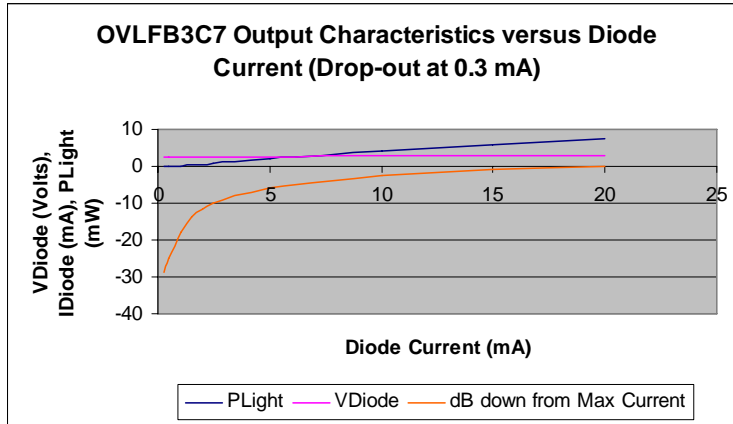


Measurement Method		Automatic	
Measurement	Value	Units	
Frequency	N/A	N/A	
Pos. Pulse Width	117.50n	S	
Neg. Pulse Width	N/A	N/A	
Rise Time	29.867n	S	
Fall Time	108.50n	S	
Pos. Duty Cycle	N/A	N/A	
Neg. Duty Cycle	N/A	N/A	
Pos. Overshoot	0.0000	%	
Neg. Overshoot	0.0000	%	
Peak to Peak	2.8800	V	
Amplitude	2.8800	V	
High	2.9600	V	
Low	80.000m	V	
Maximum	2.9600	V	
Minimum	80.000m	V	
Mean	302.78m	V	
Cycle Mean	N/A	N/A	
RMS	465.40m	V	
BurstWidth	117.50n	S	
Period	N/A	N/A	
Energy	1.0826u		
CEnergy	N/A	N/A	
ACRMS	353.40m	V	
CRMS	N/A	N/A	

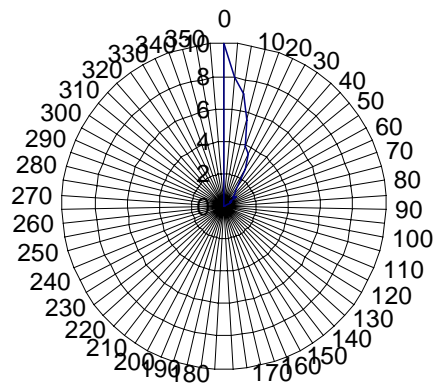
4.2.3. OVLFB3C7 [13]

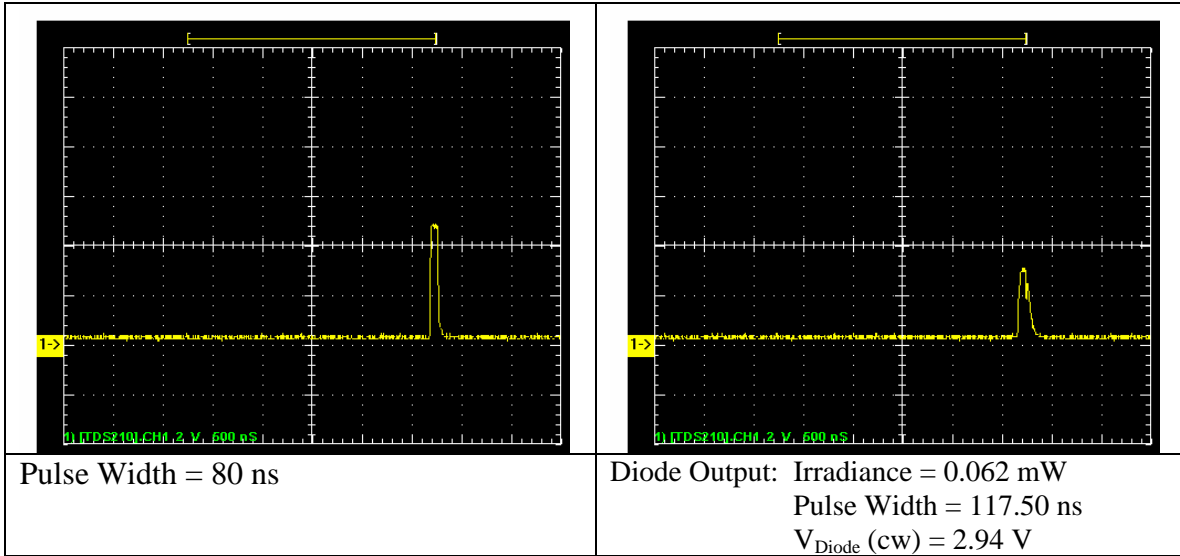
Specifications

Colour	Wavelength (nm)	Luminous Intensity (Typ.) mcd @ If(mA)	Viewing Angle (X2 Theta)
Blue	470	1350 20	30 degrees



Using the Power Measured at Ten Centimeters From the OVLFB3C7 LED at Zero Degrees, This is a Plot of the Distance Required to Measure the Same Power Level at Angles around the LED



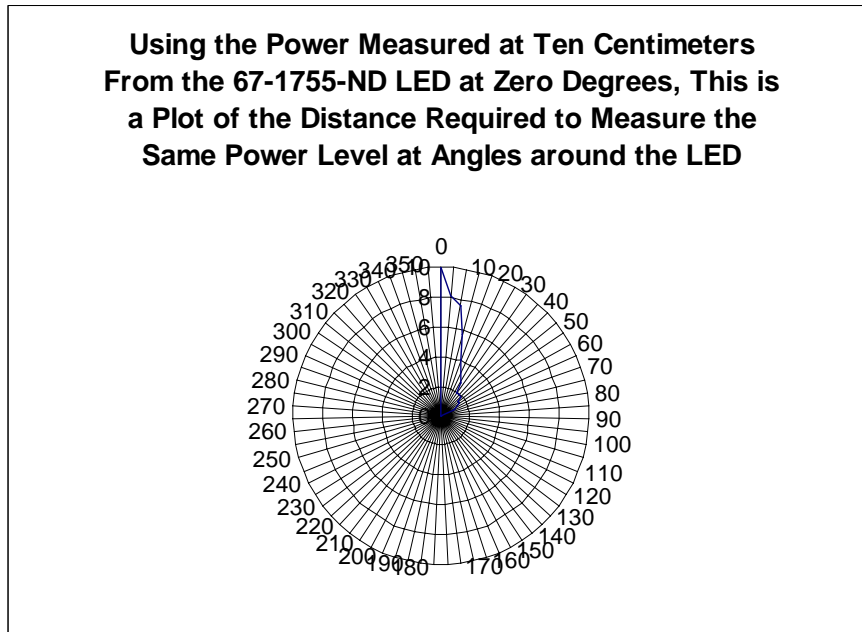
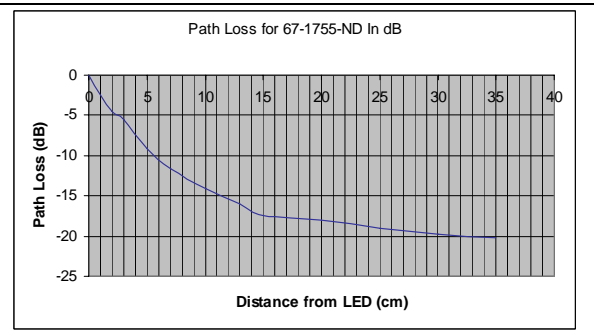
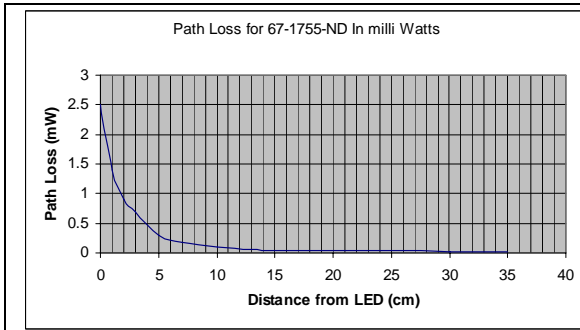
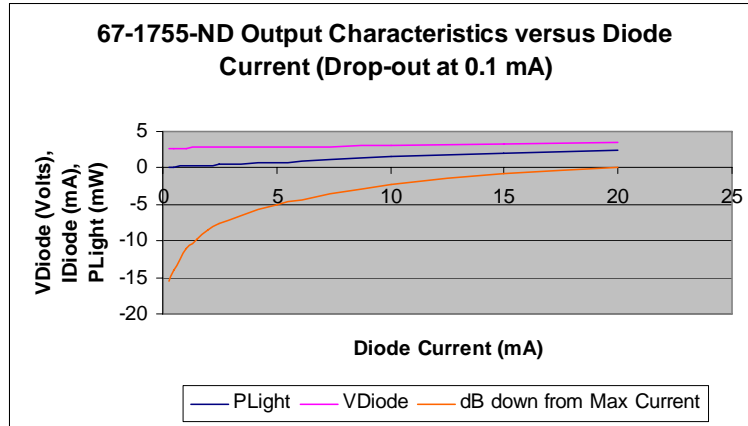


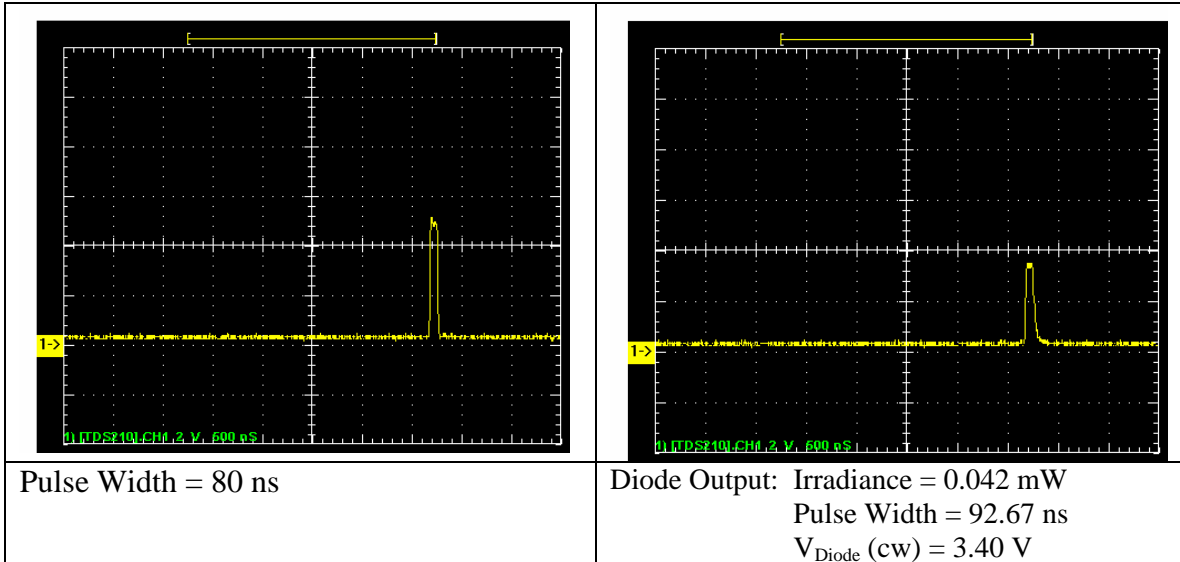
Measurement Method	Automatic	
Measurement	Value	Units
Frequency	N/A	N/A
Pos. Pulse Width	117.50n	S
Neg. Pulse Width	N/A	N/A
Rise Time	29.867n	S
Fall Time	108.50n	S
Pos. Duty Cycle	N/A	N/A
Neg. Duty Cycle	N/A	N/A
Pos. Overshoot	0.0000	%
Neg. Overshoot	0.0000	%
Peak to Peak	2.8800	V
Amplitude	2.8800	V
High	2.9600	V
Low	80.000m	V
Maximum	2.9600	V
Minimum	80.000m	V
Mean	302.78m	V
Cycle Mean	N/A	N/A
RMS	465.40m	V
BurstWidth	117.50n	S
Period	N/A	N/A
Energy	1.0826u	
CEnergy	N/A	N/A
ACRMS	353.40m	V
CRMS	N/A	N/A

4.2.4. 67-1755-ND [13]

Specifications

Colour	Wavelength (nm)	Luminous Intensity (Typ.) mcd @ If(mA)	Viewing Angle (X2 Theta)
Green	502	1500 25	30 degrees



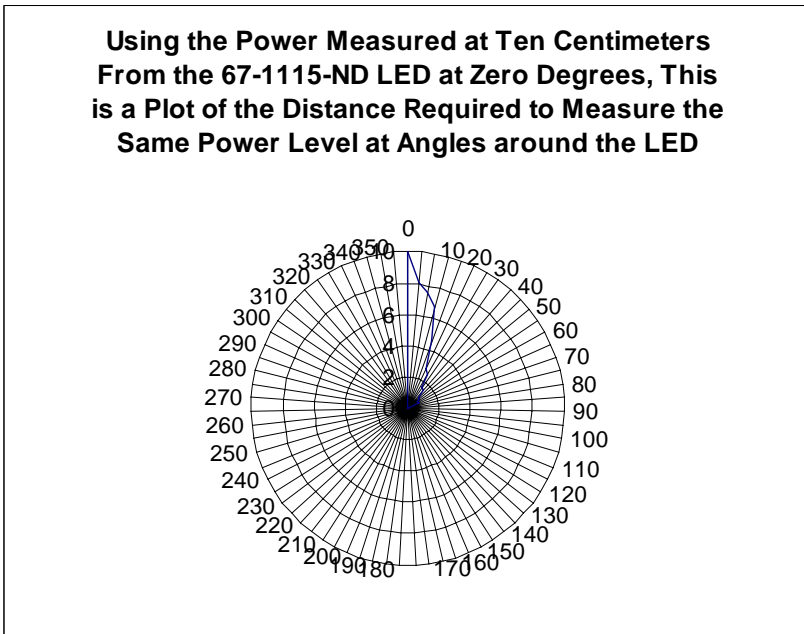
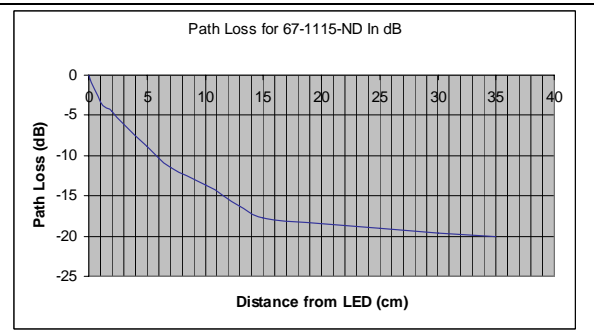
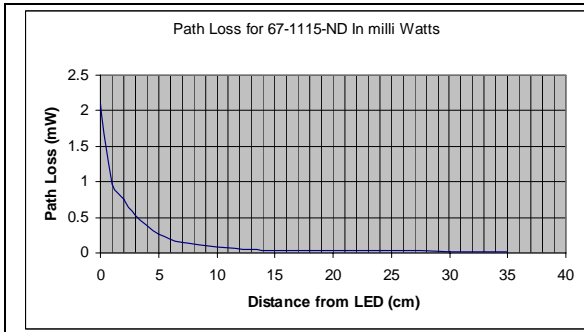
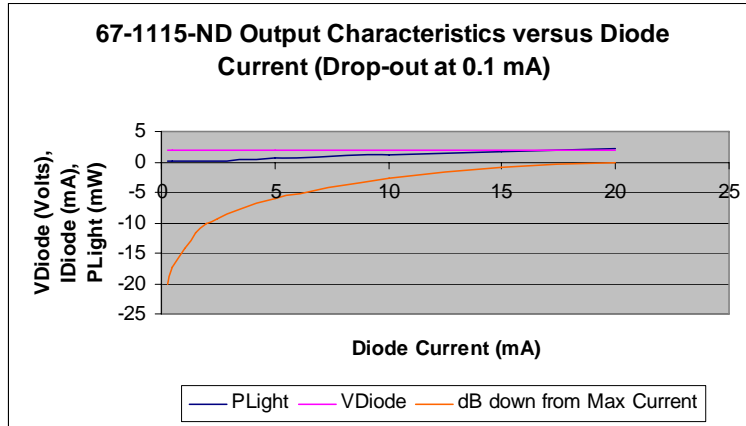


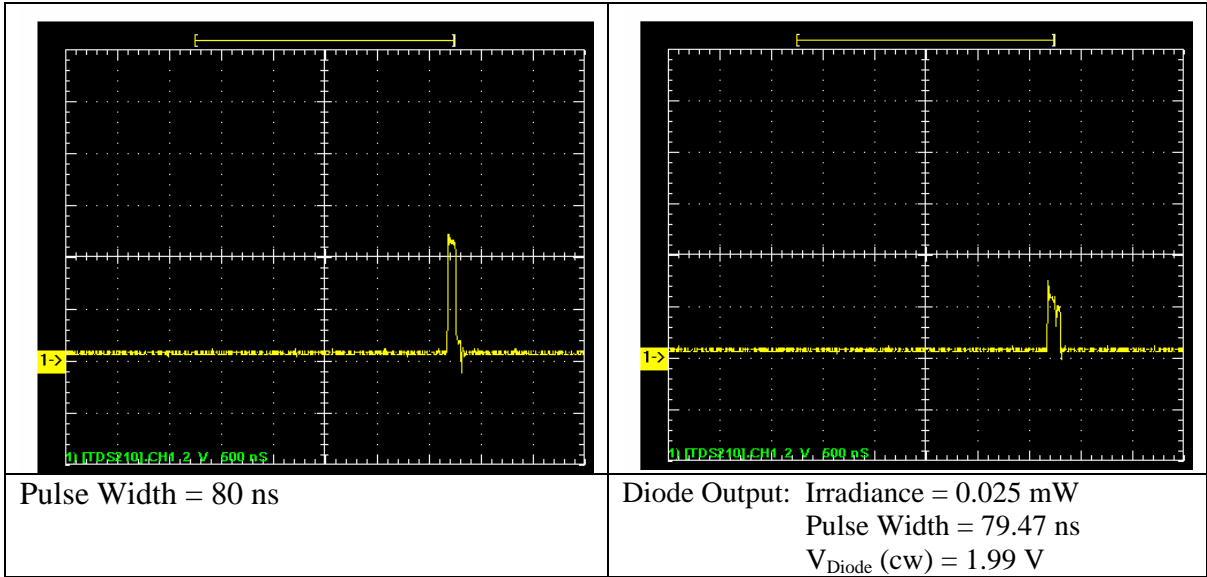
Measurement Method		Automatic	
Measurement	Value	Units	
Frequency	N/A	N/A	
Pos. Pulse Width	92.667n	S	
Neg. Pulse Width	N/A	N/A	
Rise Time	21.600n	S	
Fall Time	68.400n	S	
Pos. Duty Cycle	N/A	N/A	
Neg. Duty Cycle	N/A	N/A	
Pos. Overshoot	0.0000	%	
Neg. Overshoot	0.0000	%	
Peak to Peak	3.3600	V	
Amplitude	3.3600	V	
High	3.4400	V	
Low	80.000m	V	
Maximum	3.4400	V	
Minimum	80.000m	V	
Mean	302.71m	V	
Cycle Mean	N/A	N/A	
RMS	490.67m	V	
BurstWidth	92.667n	S	
Period	N/A	N/A	
Energy	1.2033u		
CEnergy	N/A	N/A	
ACRMS	386.12m	V	
CRMS	N/A	N/A	

4.2.5. 67-1115-ND [13]

Specifications

Colour	Wavelength (nm)	Luminous Intensity (Typ.) mcd @ If(mA)	Viewing Angle (X2 Theta)
Sup. Yellow	590	1000 30	30 degrees





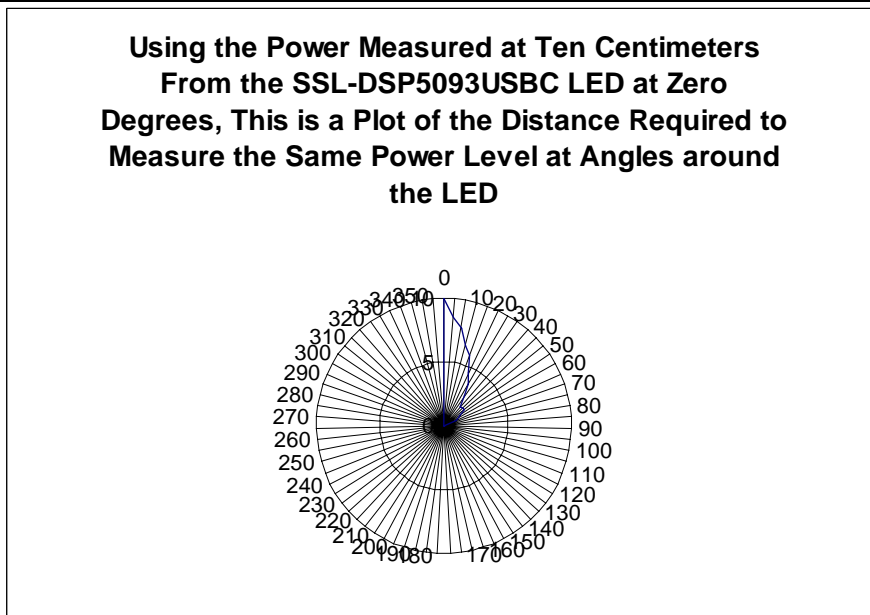
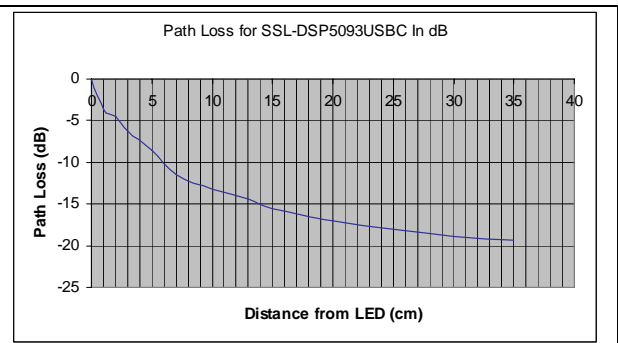
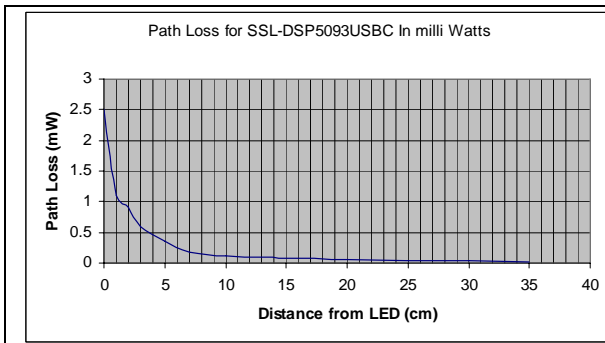
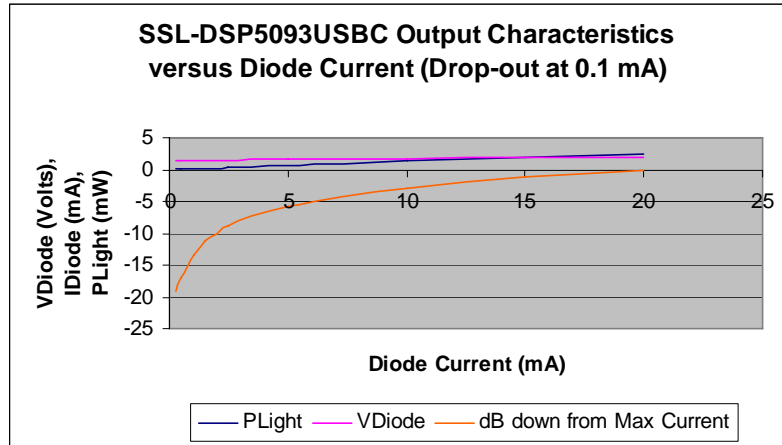
✓ S210].Data.Waveforms.C

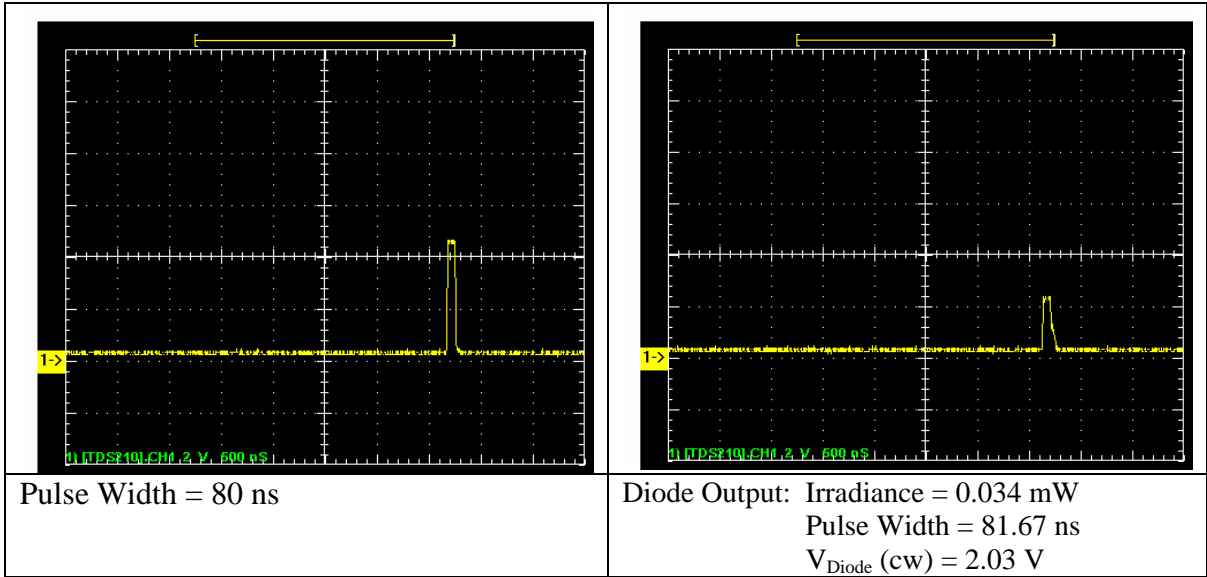
Measurement Method	Automatic	
Measurement	Value	Units
Frequency	N/A	N/A
Pos. Pulse Width	79.472n	S
Neg. Pulse Width	N/A	N/A
Rise Time	21.440n	S
Fall Time	120.83n	S
Pos. Duty Cycle	N/A	N/A
Neg. Duty Cycle	N/A	N/A
Pos. Overshoot	0.0000	%
Neg. Overshoot	0.0000	%
Peak to Peak	3.1200	V
Amplitude	3.1200	V
High	3.0400	V
Low	-80.000m	V
Maximum	3.0400	V
Minimum	-80.000m	V
Mean	294.63m	V
Cycle Mean	N/A	N/A
RMS	420.02m	V
BurstWidth	125.97n	S
Period	N/A	N/A
Energy	881.75n	
CEnergy	N/A	N/A
ACRMS	299.30m	V
CRMS	N/A	N/A

4.2.6. SSL-DSP5093USBC [13]

Specifications

Colour	Wavelength (nm)	Luminous Intensity (Typ.) mcd @ If(mA)	Viewing Angle (X2 Theta)
Blue	470	2500 25	30 degrees





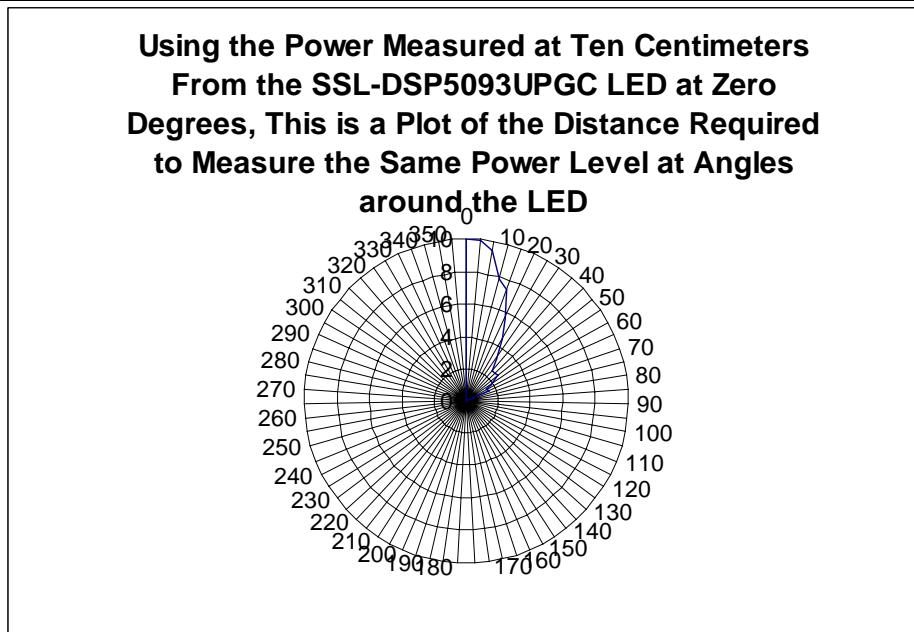
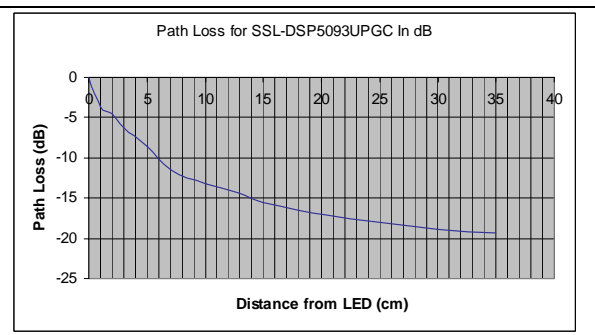
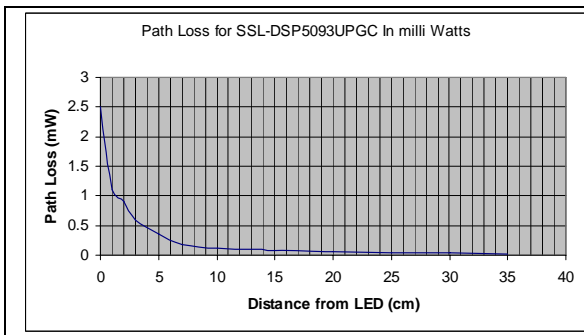
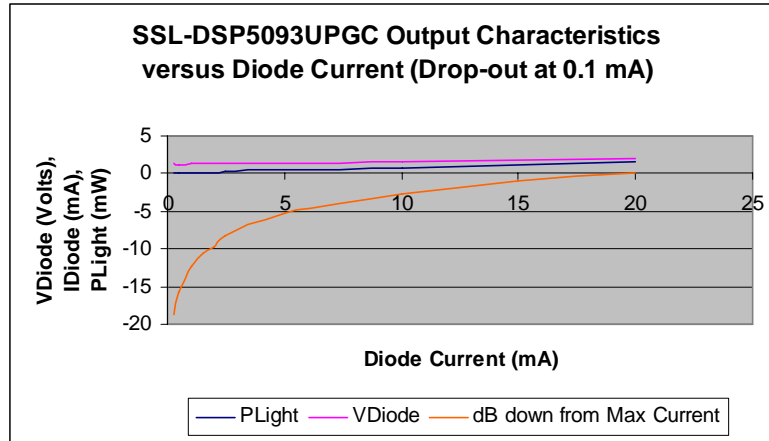
✓ S210].Data.Waveforms.C

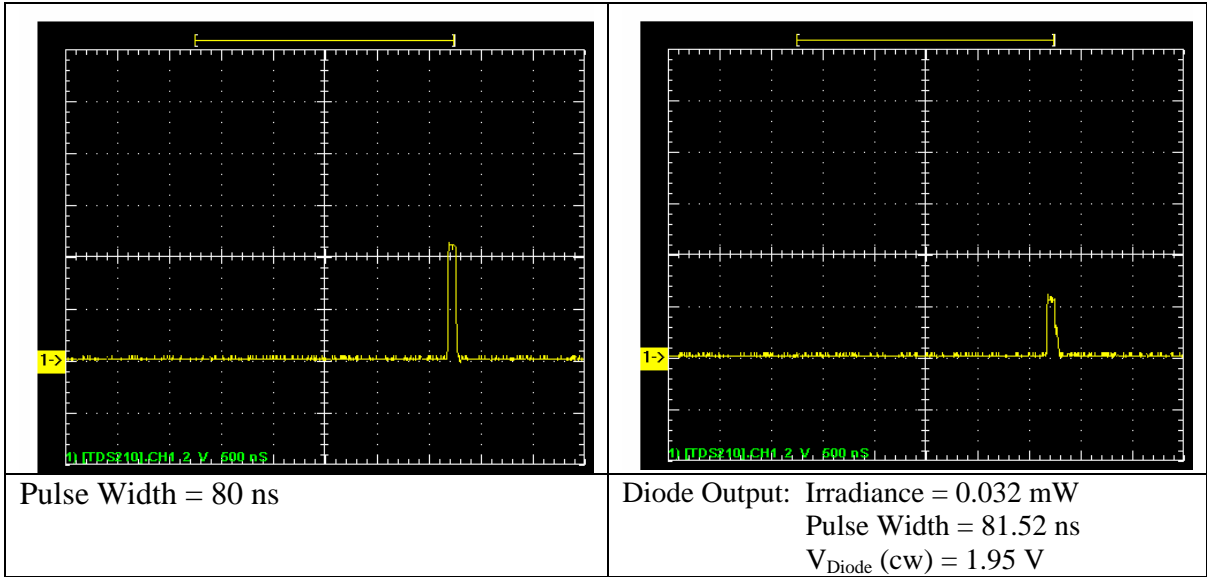
Measurement Method	Automatic	
Measurement	Value	Units
Frequency	N/A	N/A
Pos. Pulse Width	81.667n	S
Neg. Pulse Width	N/A	N/A
Rise Time	10.740n	S
Fall Time	59.300n	S
Pos. Duty Cycle	N/A	N/A
Neg. Duty Cycle	N/A	N/A
Pos. Overshoot	0.0000	%
Neg. Overshoot	0.0000	%
Peak to Peak	2.3200	V
Amplitude	2.3200	V
High	2.4000	V
Low	80.000m	V
Maximum	2.4000	V
Minimum	80.000m	V
Mean	281.30m	V
Cycle Mean	N/A	N/A
RMS	382.92m	V
BurstWidth	95.667n	S
Period	N/A	N/A
Energy	732.86n	
CEnergy	N/A	N/A
ACRMS	259.75m	V
CRMS	N/A	N/A

4.2.7. SSL-DSP5093UPGC [13]

Specifications

Colour	Wavelength (nm)	Luminous Intensity (Typ.) mcd @ If(mA)	Viewing Angle (X2 Theta)
Green	525	3500 25	30 degrees



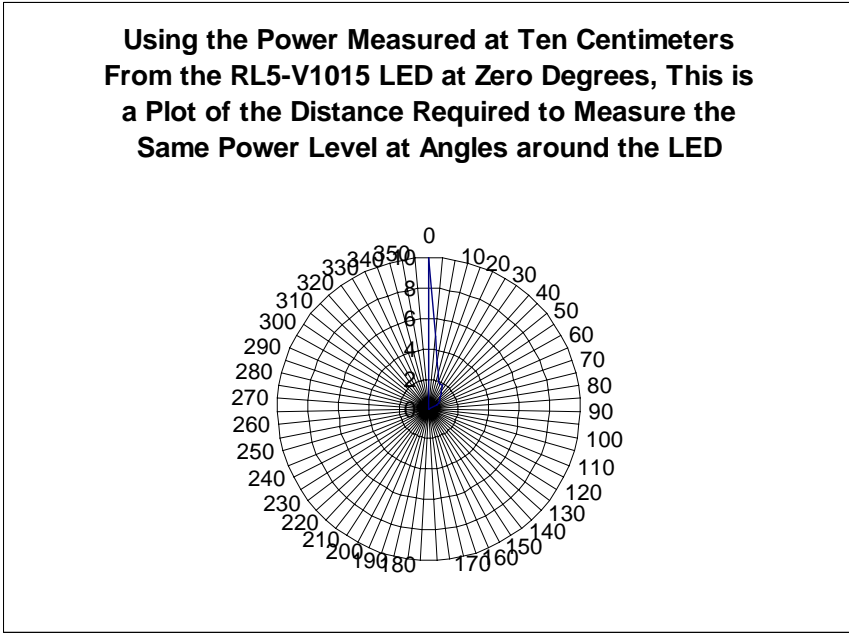
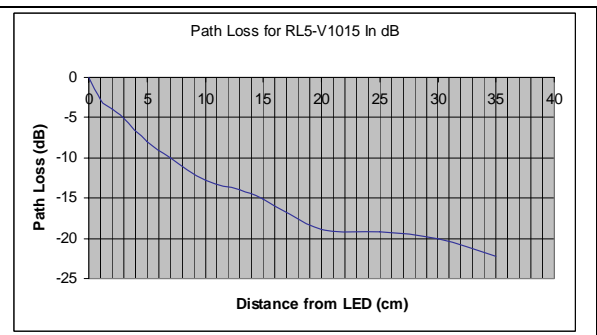
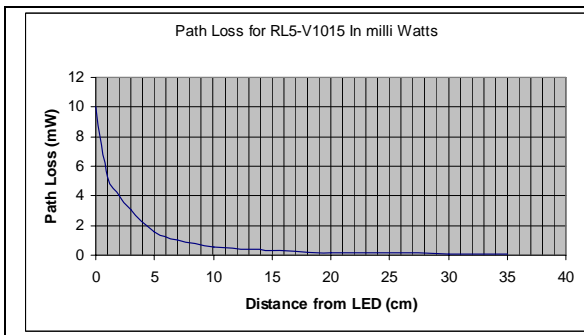
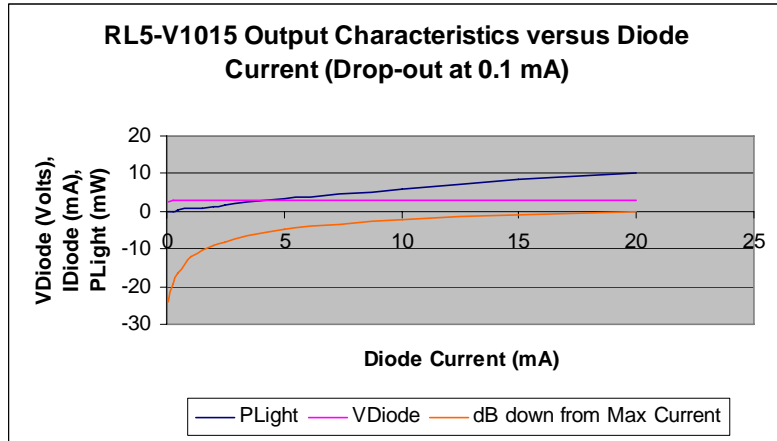


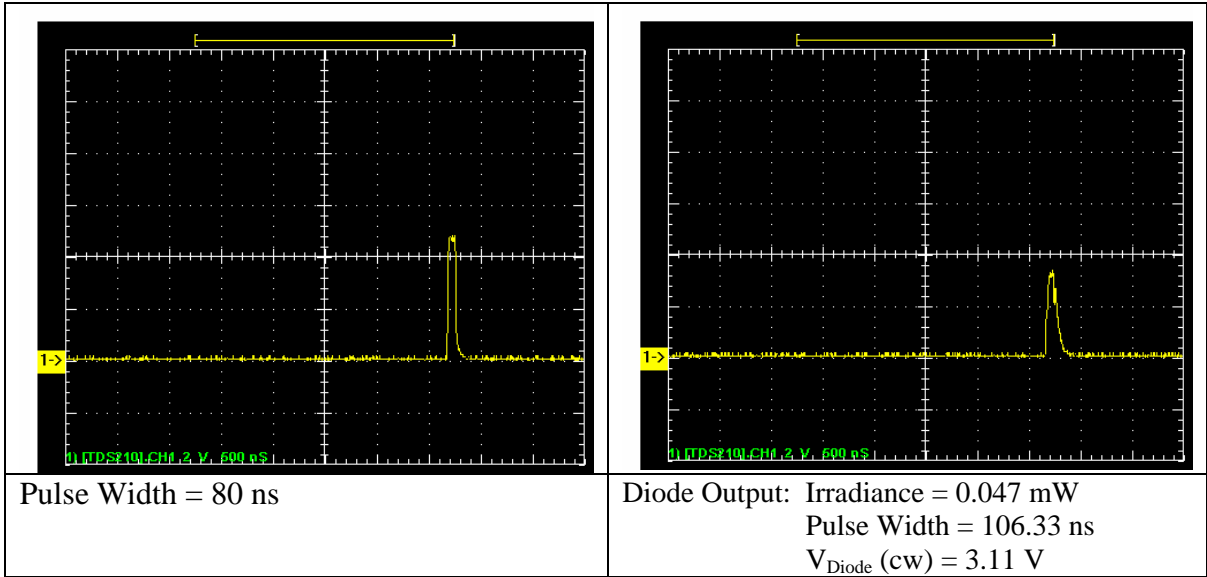
Measurement Method	Automatic	
Measurement	Value	Units
Frequency	10.769M	Hz
Pos. Pulse Width	81.524n	S
Neg. Pulse Width	11.333n	S
Rise Time	10.500n	S
Fall Time	48.000n	S
Pos. Duty Cycle	877.95m	%
Neg. Duty Cycle	122.05m	%
Pos. Overshoot	0.0000	%
Neg. Overshoot	0.0000	%
Peak to Peak	2.4000	V
Amplitude	2.4000	V
High	2.3200	V
Low	-80.000m	V
Maximum	2.3200	V
Minimum	-80.000m	V
Mean	83.329m	V
Cycle Mean	1.9327	V
RMS	286.96m	V
BurstWidth	94.857n	S
Period	92.857n	S
Energy	411.56n	
CEnergy	370.23n	
ACRMS	274.59m	V
CRMS	1.9968	V

4.2.8. RL5-V1015 [14]

Specifications

Colour	Wavelength (nm)	Luminous Intensity (Typ.) mcd	Viewing Angle (X2 Theta)
Violet	420	1000	15 degrees





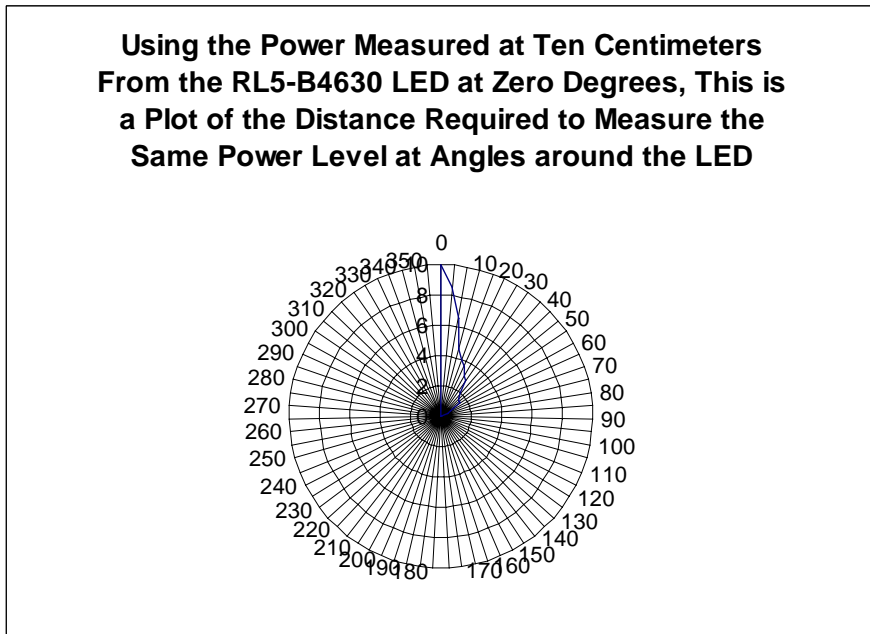
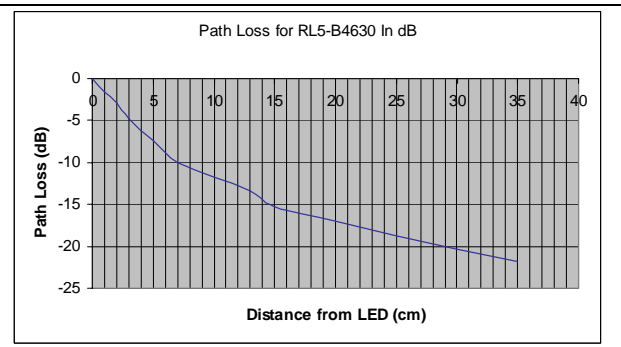
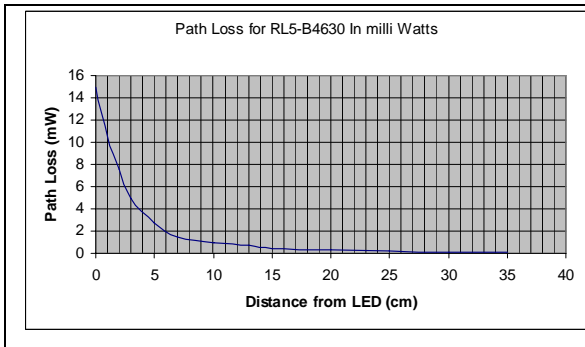
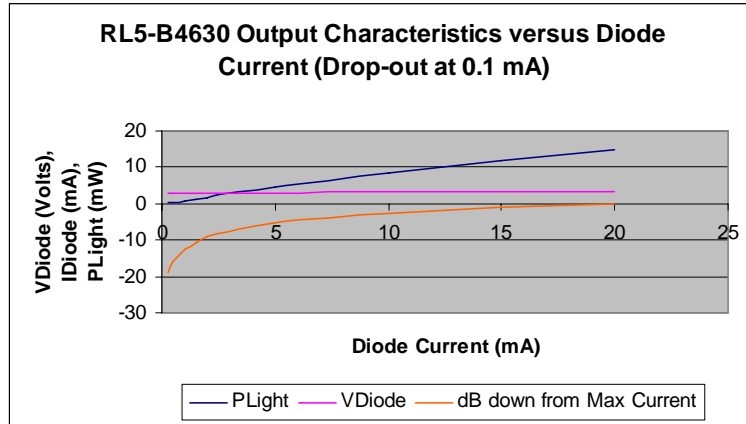
✓ S210].Data.Waveforms.C

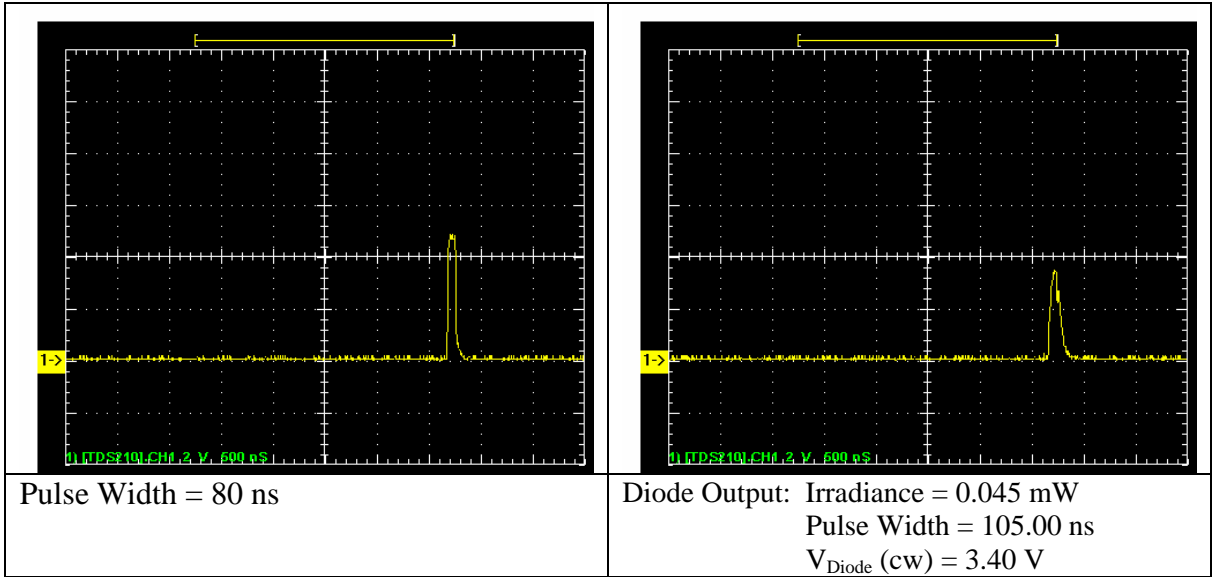
Measurement Method	Automatic	
Measurement	Value	Units
Frequency	N/A	N/A
Pos. Pulse Width	106.33n	S
Neg. Pulse Width	N/A	N/A
Rise Time	32.400n	S
Fall Time	106.60n	S
Pos. Duty Cycle	N/A	N/A
Neg. Duty Cycle	N/A	N/A
Pos. Overshoot	0.0000	%
Neg. Overshoot	0.0000	%
Peak to Peak	3.3600	V
Amplitude	3.3600	V
High	3.2800	V
Low	-80.000m	V
Maximum	3.2800	V
Minimum	-80.000m	V
Mean	106.17m	V
Cycle Mean	N/A	N/A
RMS	410.86m	V
BurstWidth	106.33n	S
Period	N/A	N/A
Energy	843.68n	
CEnergy	N/A	N/A
ACRMS	396.90m	V
CRMS	N/A	N/A

4.2.9. RL5-B4630 [14]

Specifications

Colour	Wavelength (nm)	Luminous Intensity (Typ.) mcd	Viewing Angle (X2 Theta)
Blue	472	4600	30 degrees



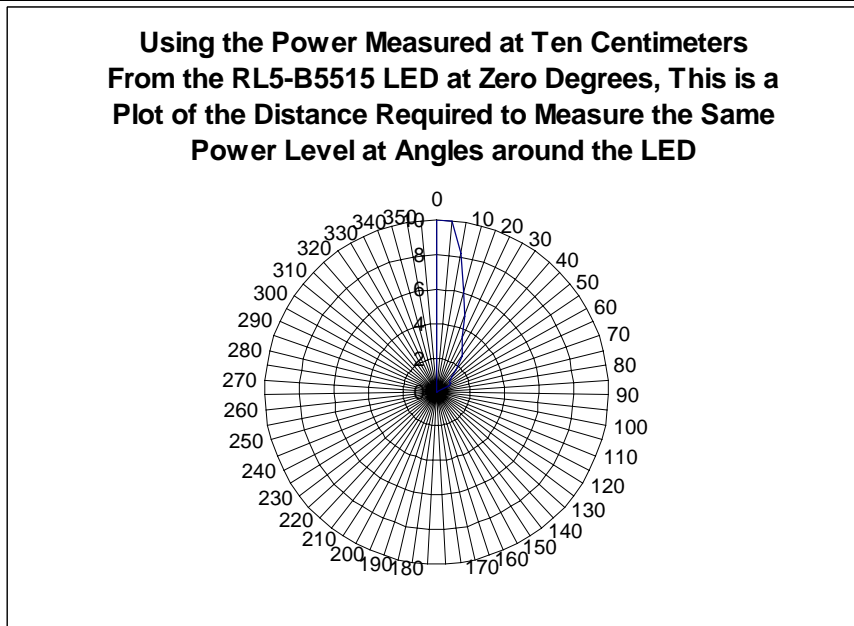
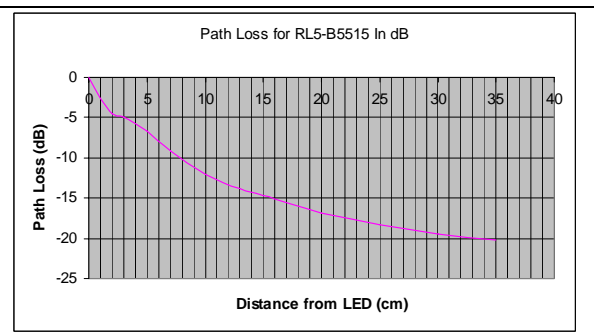
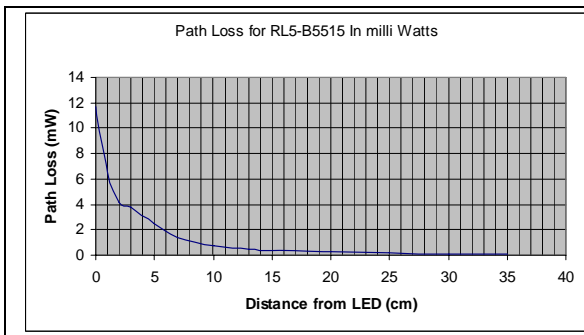
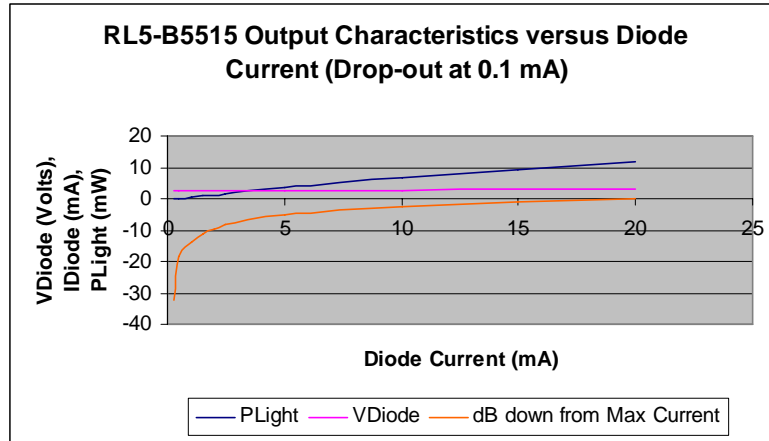


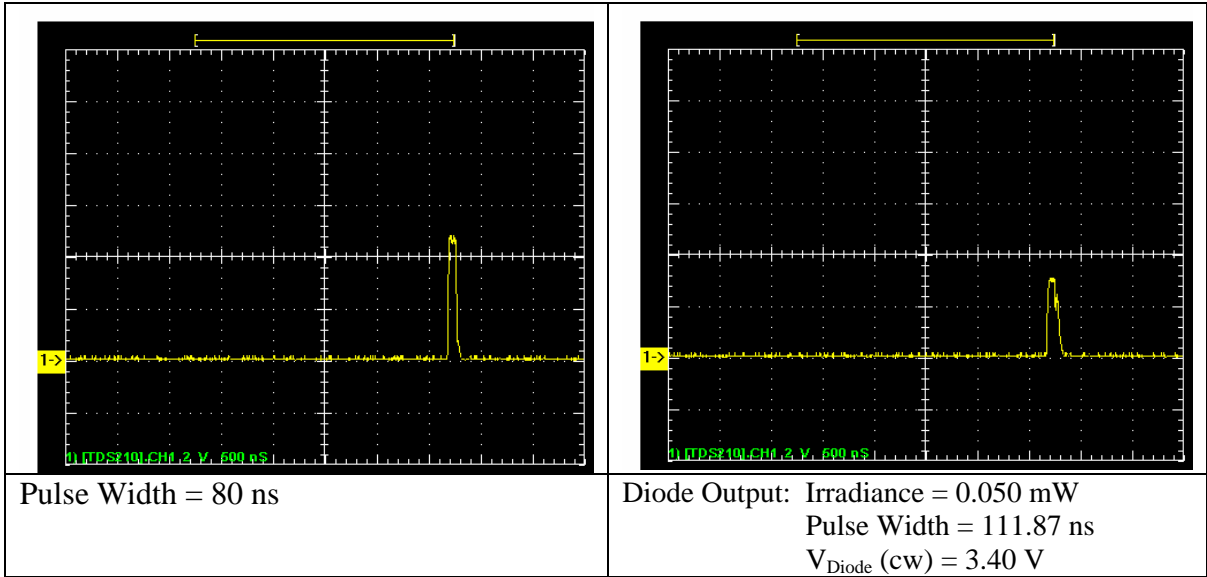
		✓ S210].Data.Waveforms.C
Measurement Method	Automatic	
Measurement	Value	Units
Frequency	N/A	N/A
Pos. Pulse Width	105.00n	S
Neg. Pulse Width	N/A	N/A
Rise Time	42.667n	S
Fall Time	90.667n	S
Pos. Duty Cycle	N/A	N/A
Neg. Duty Cycle	N/A	N/A
Pos. Overshoot	0.0000	%
Neg. Overshoot	0.0000	%
Peak to Peak	3.5200	V
Amplitude	3.5200	V
High	3.4400	V
Low	-80.000m	V
Maximum	3.4400	V
Minimum	-80.000m	V
Mean	110.52m	V
Cycle Mean	N/A	N/A
RMS	427.67m	V
BurstWidth	105.00n	S
Period	N/A	N/A
Energy	914.16n	
CEnergy	N/A	N/A
ACRMS	413.14m	V
CRMS	N/A	N/A

4.2.10. RL5-B5515 [14]

Specifications

Colour	Wavelength (nm)	Luminous Intensity (Typ.) mcd	Viewing Angle (X2 Theta)
Blue	470	5500	15 degrees



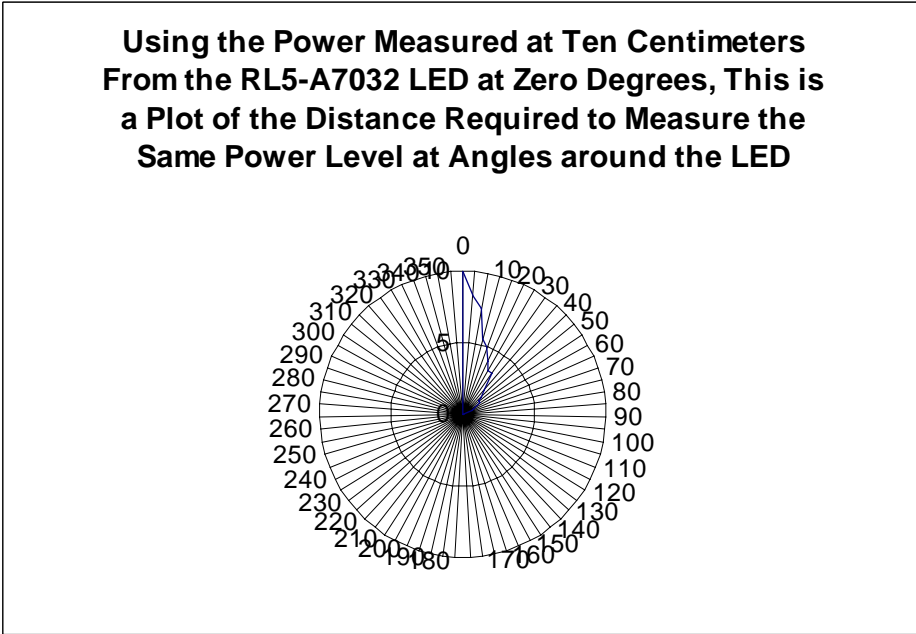
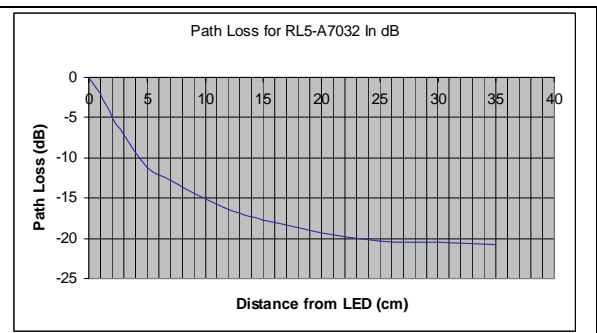
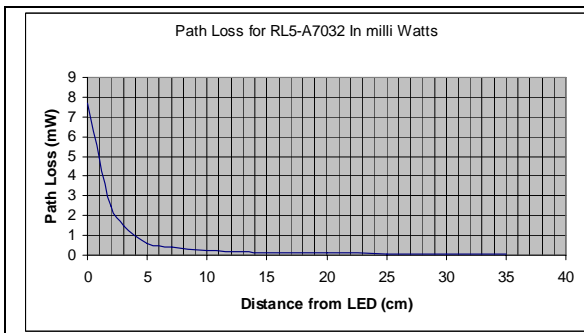
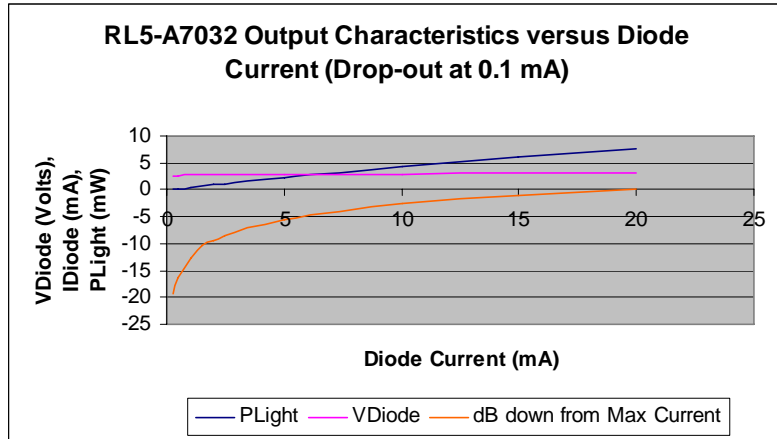


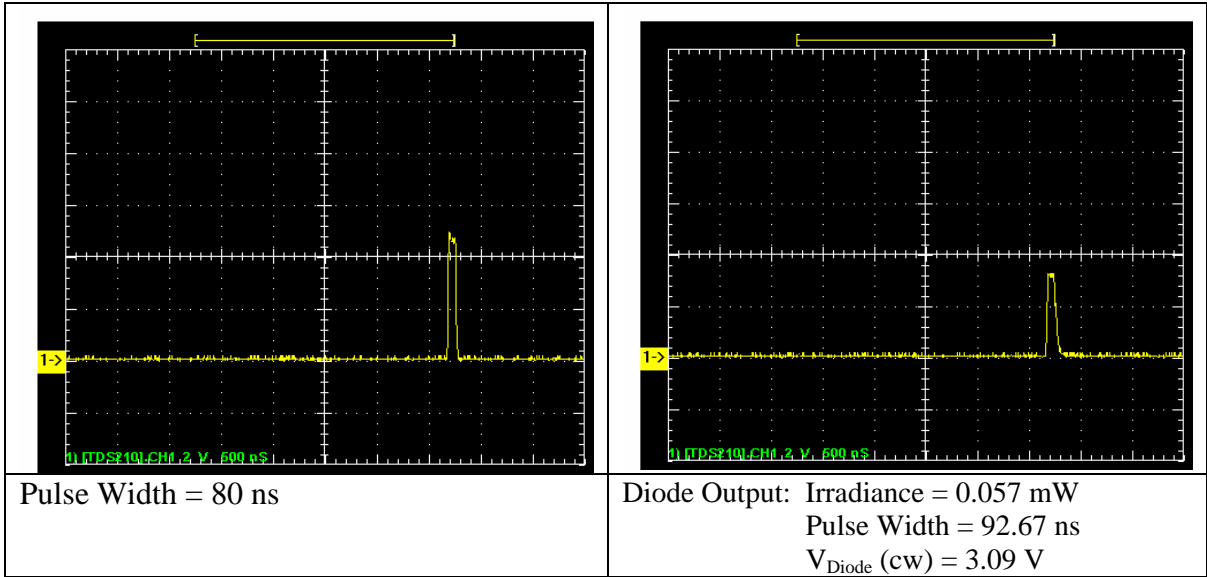
		✓ S210].Data.Waveforms.C	
Measurement Method	Automatic		
Measurement	Value	Units	
Frequency	N/A	N/A	
Pos. Pulse Width	111.87n	S	
Neg. Pulse Width	N/A	N/A	
Rise Time	22.300n	S	
Fall Time	70.300n	S	
Pos. Duty Cycle	N/A	N/A	
Neg. Duty Cycle	N/A	N/A	
Pos. Overshoot	0.0000	%	
Neg. Overshoot	0.0000	%	
Peak to Peak	3.1200	V	
Amplitude	3.1200	V	
High	3.0400	V	
Low	-80.000m	V	
Maximum	3.0400	V	
Minimum	-80.000m	V	
Mean	101.26m	V	
Cycle Mean	N/A	N/A	
RMS	400.72m	V	
BurstWidth	114.53n	S	
Period	N/A	N/A	
Energy	802.55n		
CEnergy	N/A	N/A	
ACRMS	387.71m	V	
CRMS	N/A	N/A	

4.2.11. RL5-A7032 [14]

Specifications

Colour	Wavelength (nm)	Luminous Intensity (Typ.) mcd	Viewing Angle (X2 Theta)
Aqua	507	7000	32 degrees





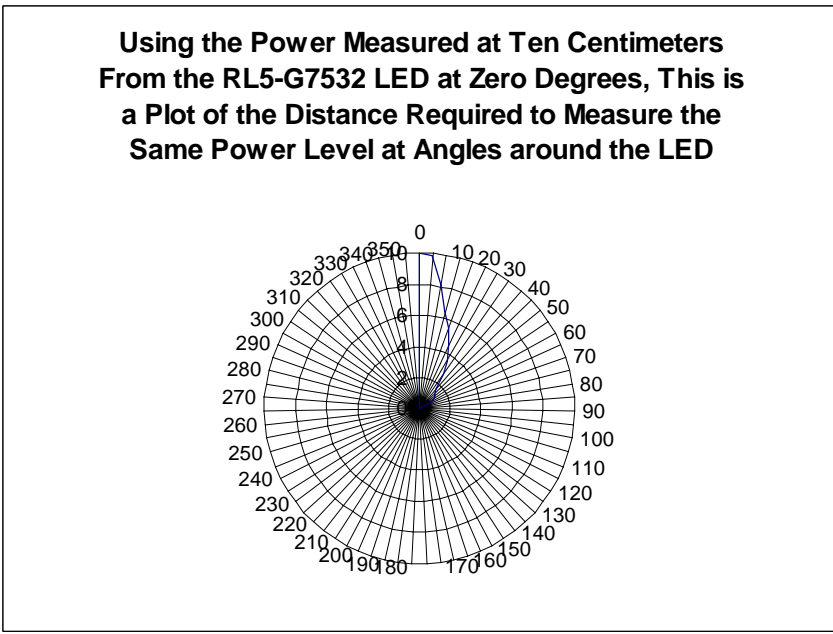
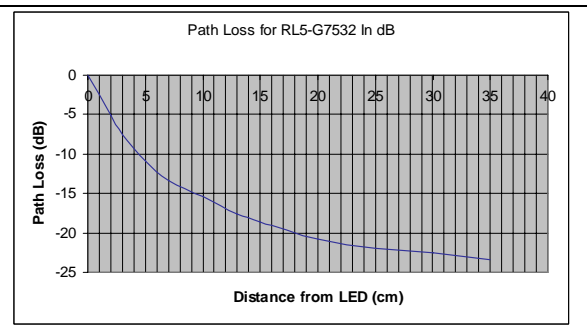
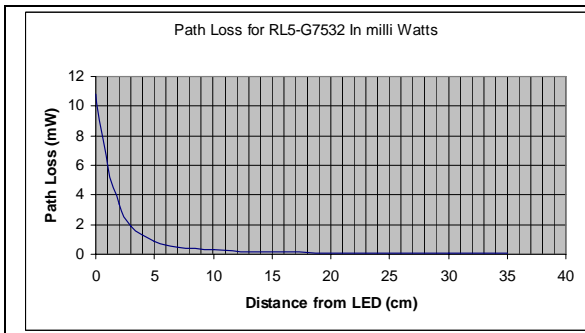
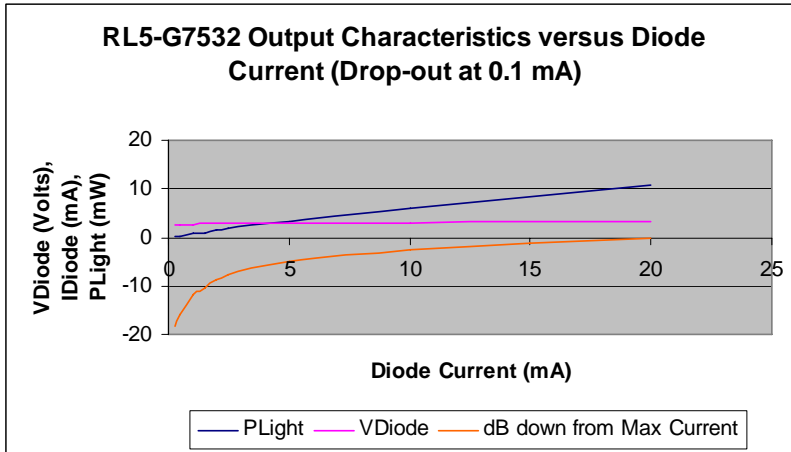
✓ S210].Data.Waveforms.C

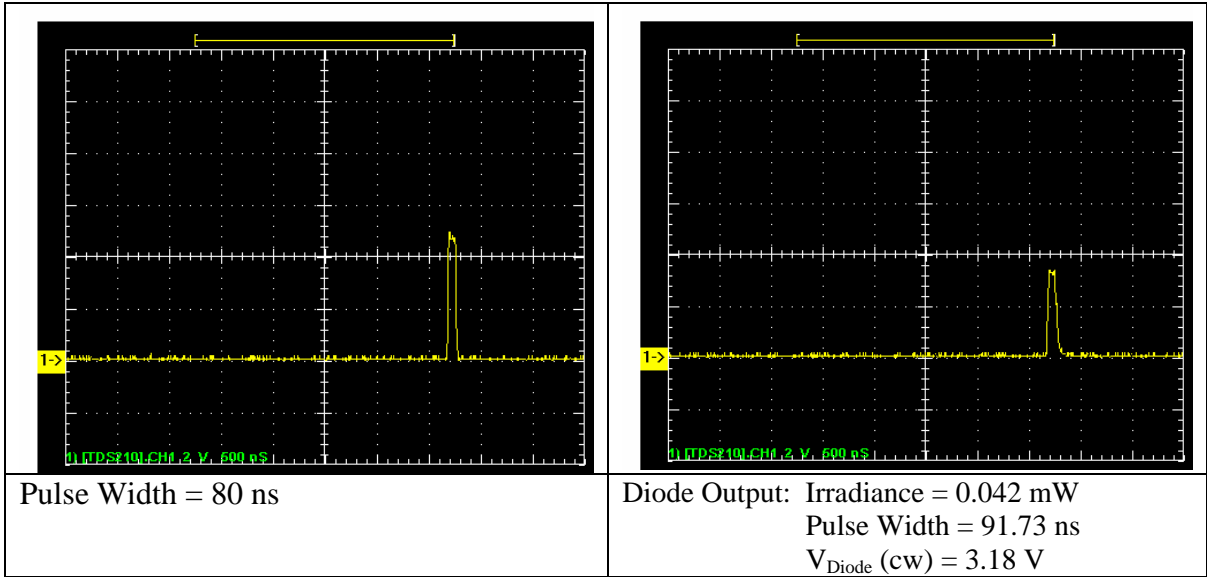
Measurement Method	Automatic	
Measurement	Value	Units
Frequency	N/A	N/A
Pos. Pulse Width	92.667n	S
Neg. Pulse Width	N/A	N/A
Rise Time	20.767n	S
Fall Time	50.700n	S
Pos. Duty Cycle	N/A	N/A
Neg. Duty Cycle	N/A	N/A
Pos. Overshoot	0.0000	%
Neg. Overshoot	0.0000	%
Peak to Peak	3.3600	V
Amplitude	3.3600	V
High	3.2800	V
Low	-80.000m	V
Maximum	3.2800	V
Minimum	-80.000m	V
Mean	94.230m	V
Cycle Mean	N/A	N/A
RMS	398.04m	V
BurstWidth	92.667n	S
Period	N/A	N/A
Energy	791.88n	
CEnergy	N/A	N/A
ACRMS	386.73m	V
CRMS	N/A	N/A

4.2.12. RL5-G7532 [14]

Specifications

Colour	Wavelength (nm)	Luminous Intensity (Typ.) mcd	Viewing Angle (X2 Theta)
Green	525	7500	32 degrees



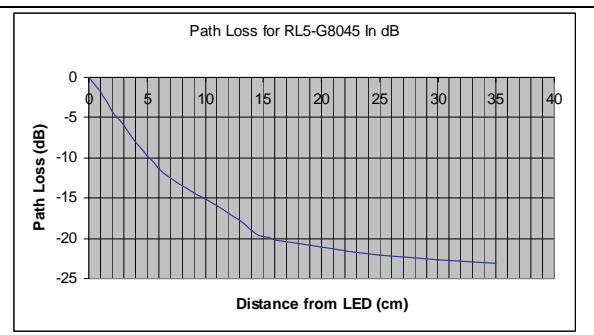
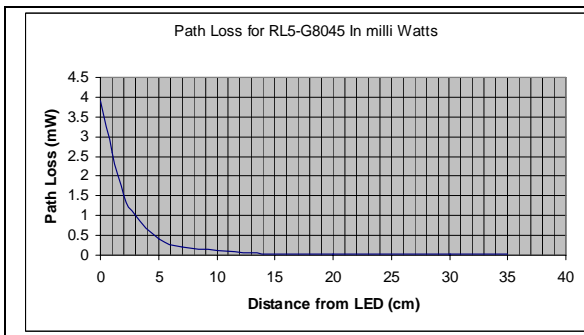
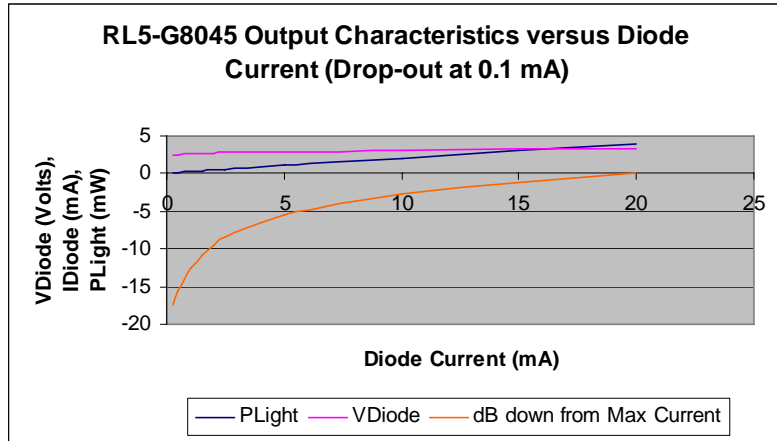


Measurement Method	Automatic	
Measurement	Value	Units
Frequency	N/A	N/A
Pos. Pulse Width	91.733n	S
Neg. Pulse Width	N/A	N/A
Rise Time	21.167n	S
Fall Time	52.100n	S
Pos. Duty Cycle	N/A	N/A
Neg. Duty Cycle	N/A	N/A
Pos. Overshoot	0.0000	%
Neg. Overshoot	0.0000	%
Peak to Peak	3.4400	V
Amplitude	3.4400	V
High	3.3600	V
Low	-80.000m	V
Maximum	3.3600	V
Minimum	-80.000m	V
Mean	99.768m	V
Cycle Mean	N/A	N/A
RMS	411.77m	V
BurstWidth	91.733n	S
Period	N/A	N/A
Energy	847.44n	
CEnergy	N/A	N/A
ACRMS	399.50m	V
CRMS	N/A	N/A

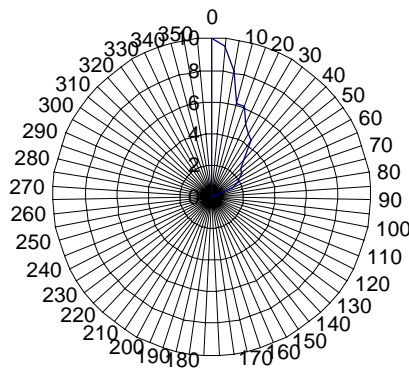
4.2.13. RL5-G8045 [14]

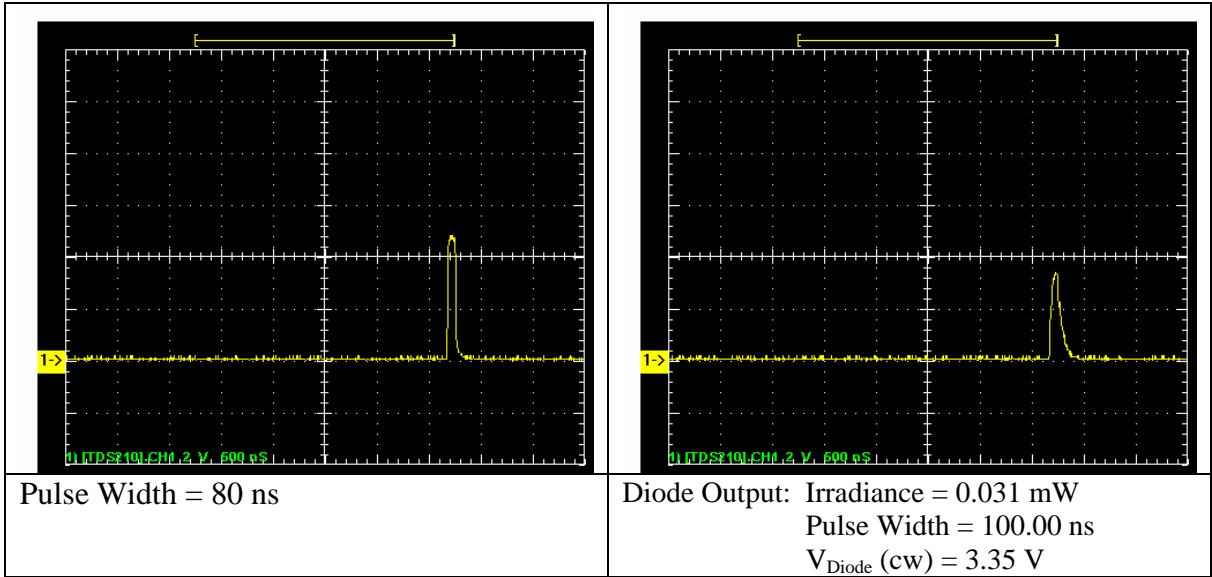
Specifications

Colour	Wavelength (nm)	Luminous Intensity (Typ.) mcd	Viewing Angle (X2 Theta)
Green	525	8000	45 degrees



Using the Power Measured at Ten Centimeters From the RL5-G8045 LED at Zero Degrees, This is a Plot of the Distance Required to Measure the Same Power Level at Angles around the LED





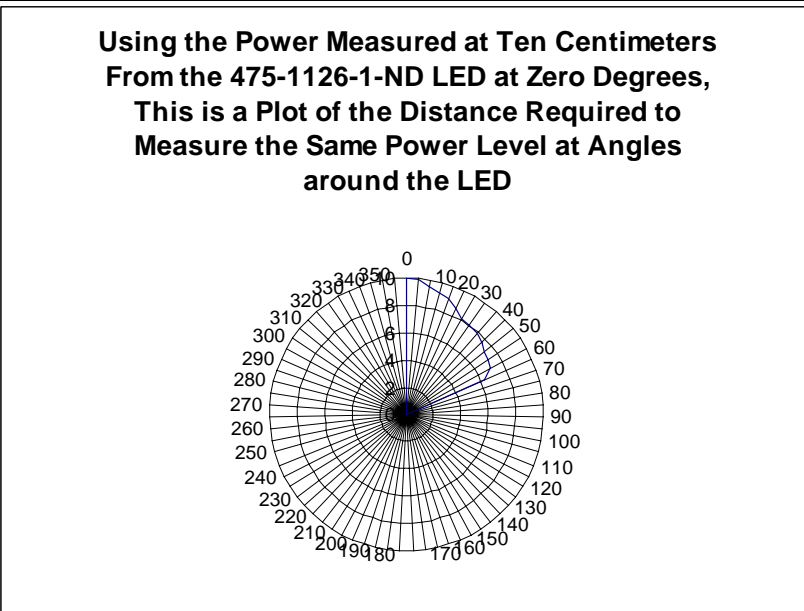
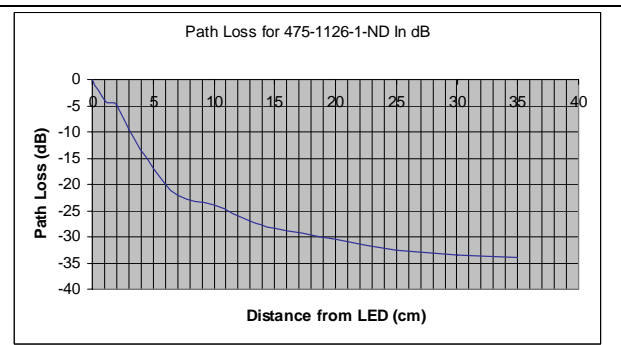
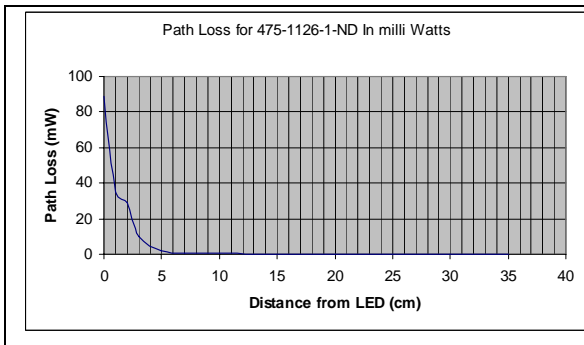
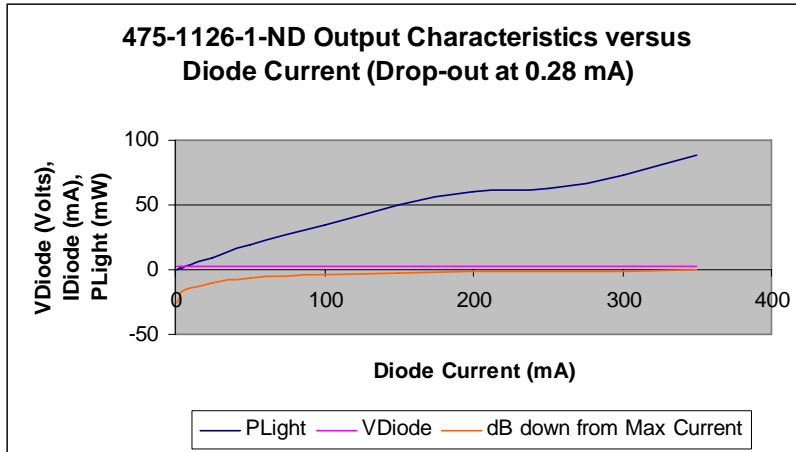
✓ S210].Data.Waveforms.C

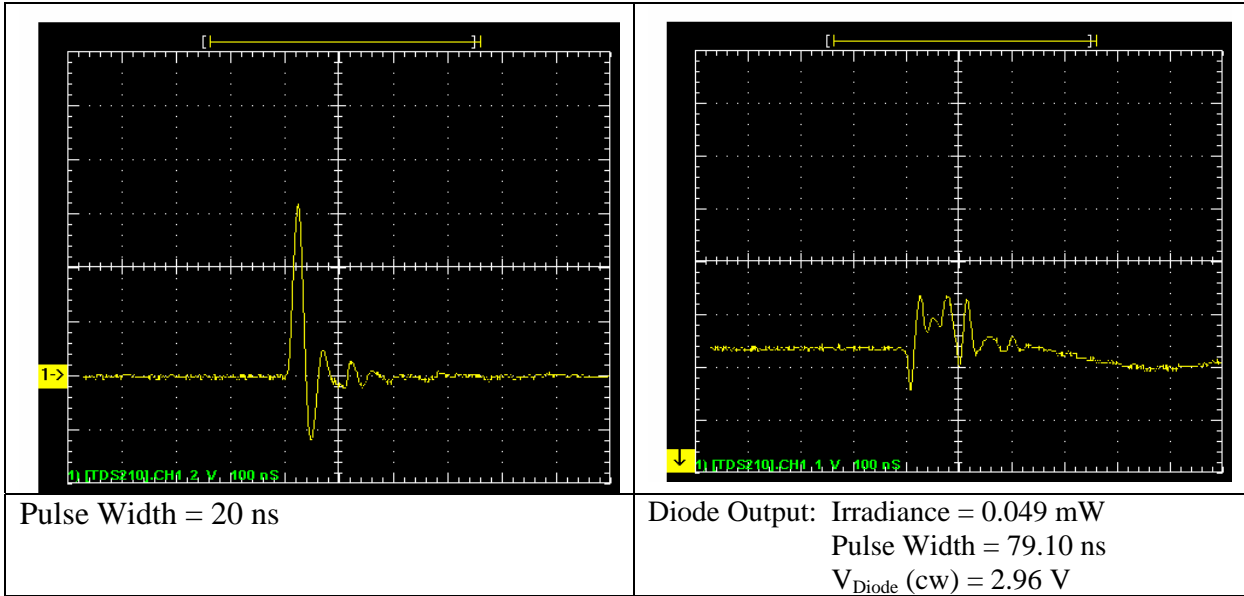
Measurement Method	Automatic	
Measurement	Value	Units
Frequency	N/A	N/A
Pos. Pulse Width	100.00n	S
Neg. Pulse Width	N/A	N/A
Rise Time	34.500n	S
Fall Time	101.55n	S
Pos. Duty Cycle	N/A	N/A
Neg. Duty Cycle	N/A	N/A
Pos. Overshoot	0.0000	%
Neg. Overshoot	0.0000	%
Peak to Peak	3.4400	V
Amplitude	3.4400	V
High	3.3600	V
Low	-80.000m	V
Maximum	3.3600	V
Minimum	-80.000m	V
Mean	103.71m	V
Cycle Mean	N/A	N/A
RMS	408.02m	V
BurstWidth	100.00n	S
Period	N/A	N/A
Energy	832.07n	
CEnergy	N/A	N/A
ACRMS	394.62m	V
CRMS	N/A	N/A

4.2.14. 475-1126-1-ND [13]

Specifications

Colour	Wavelength (nm)	Luminous Intensity (Typ.) mcd @ If(mA)	Viewing Angle (X2 Theta)
True Green	520	10,000 350	120 degrees



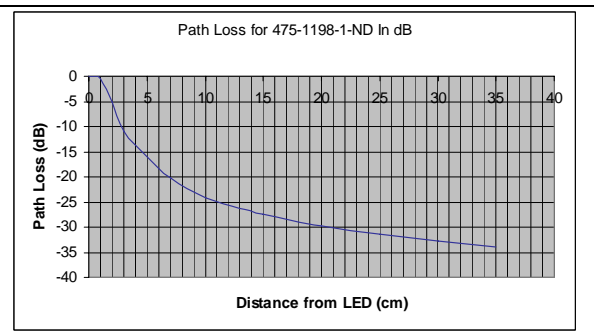
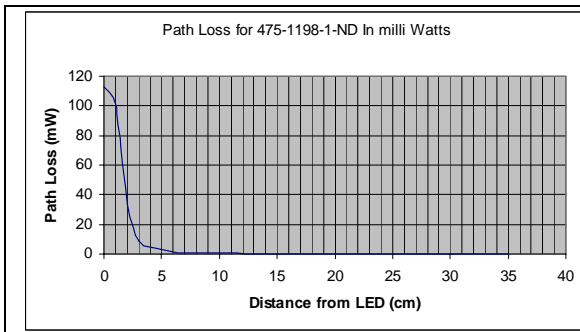
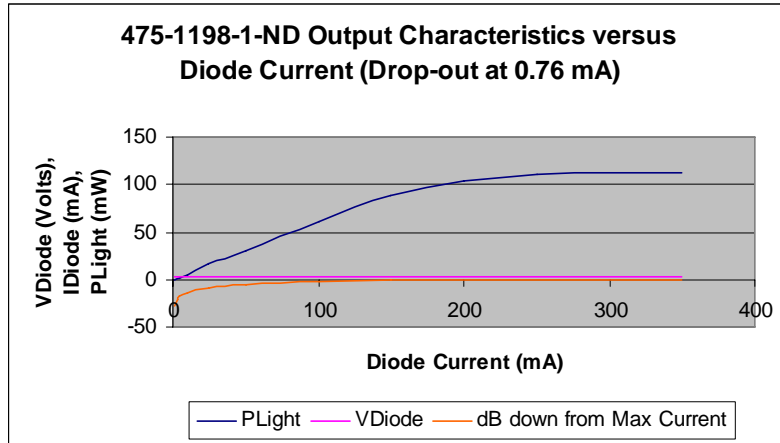


Measurement Method		Automatic	
Measurement	Value	Units	
Frequency	11.111M	Hz	
Pos. Pulse Width	79.100n	S	
Neg. Pulse Width	10.900n	S	
Rise Time	13.380n	S	
Fall Time	N/A	N/A	
Pos. Duty Cycle	878.89m	%	
Neg. Duty Cycle	121.11m	%	
Pos. Overshoot	0.0000	%	
Neg. Overshoot	0.0000	%	
Peak to Peak	1.8800	V	
Amplitude	1.8800	V	
High	3.3200	V	
Low	1.4400	V	
Maximum	3.3200	V	
Minimum	1.4400	V	
Mean	2.2420	V	
Cycle Mean	2.7665	V	
RMS	2.2586	V	
BurstWidth	194.00n	S	
Period	90.000n	S	
Energy	5.0994u		
CEnergy	701.12n		
ACRMS	270.08m	V	
CRMS	2.7911	V	

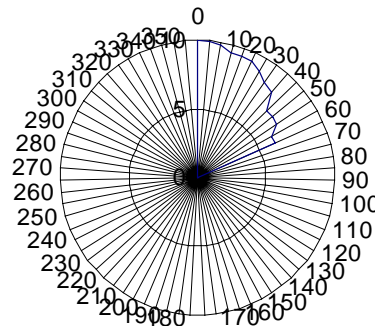
4.2.15. 475-1198-1-ND [13]

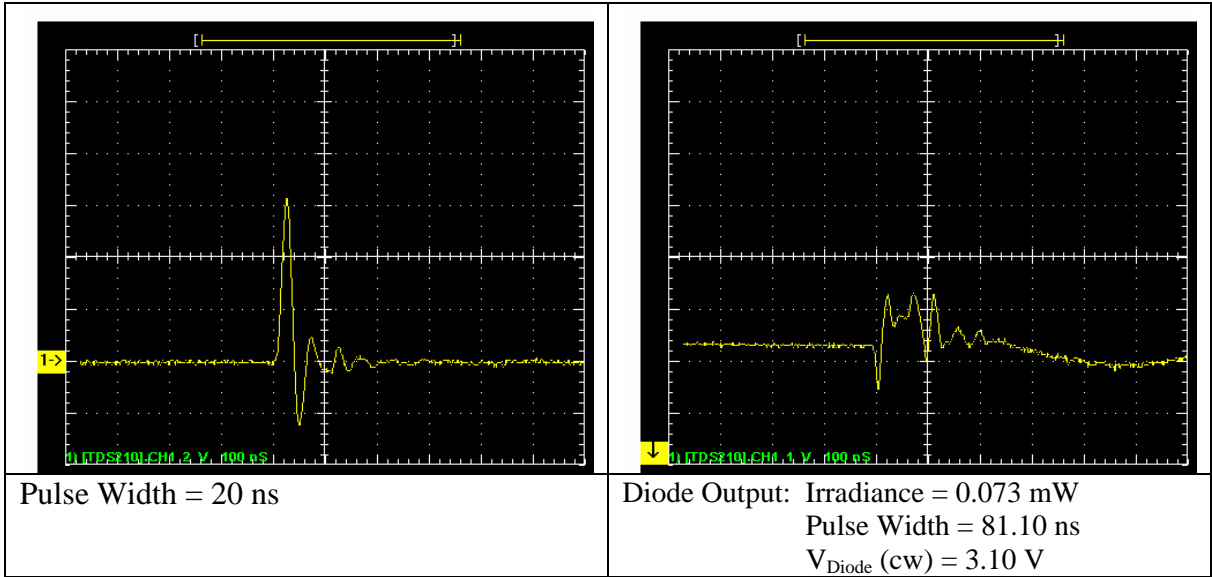
Specifications

Colour	Wavelength (nm)	Luminous Intensity (Typ.) mcd @ If(mA)	Viewing Angle (X2 Theta)
Blue	465	2700 350	120 degrees



Using the Power Measured at Ten Centimeters From the 475-1198-1-ND LED at Zero Degrees, This is a Plot of the Distance Required to Measure the Same Power Level at Angles around the LED



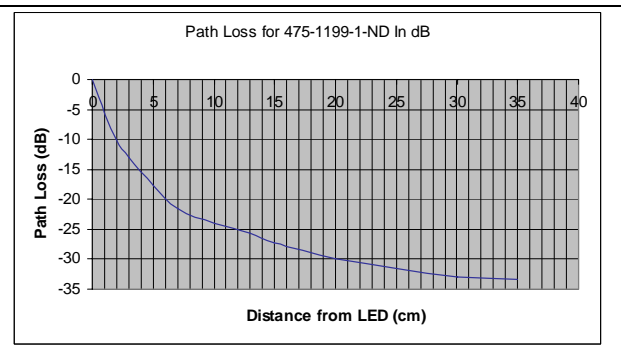
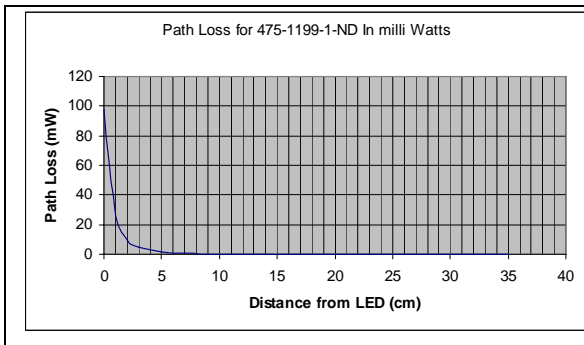
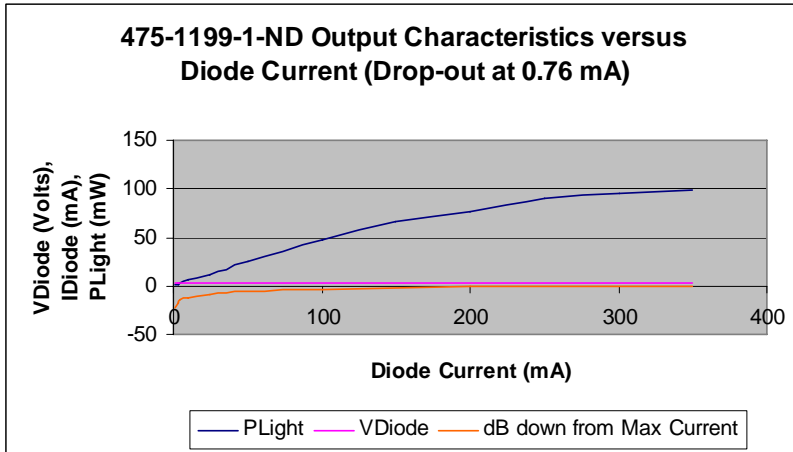


		✓ S210].Data.Waveforms.C	
Measurement Method	Automatic		
Measurement	Value	Units	
Frequency	11.025M	Hz	
Pos. Pulse Width	81.100n	S	
Neg. Pulse Width	9.6000n	S	
Rise Time	12.400n	S	
Fall Time	N/A	N/A	
Pos. Duty Cycle	894.16m	%	
Neg. Duty Cycle	105.84m	%	
Pos. Overshoot	0.0000	%	
Neg. Overshoot	0.0000	%	
Peak to Peak	1.8000	V	
Amplitude	1.8000	V	
High	3.2000	V	
Low	1.4000	V	
Maximum	3.2000	V	
Minimum	1.4000	V	
Mean	2.1853	V	
Cycle Mean	2.7412	V	
RMS	2.2039	V	
BurstWidth	238.30n	S	
Period	90.700n	S	
Energy	4.8554u		
CEnergy	692.65n		
ACRMS	282.94m	V	
CRMS	2.7635	V	

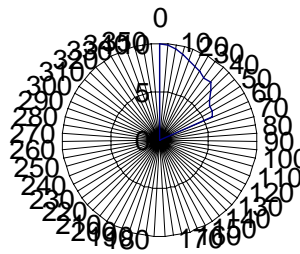
4.2.16. 475-1199-1-ND [13]

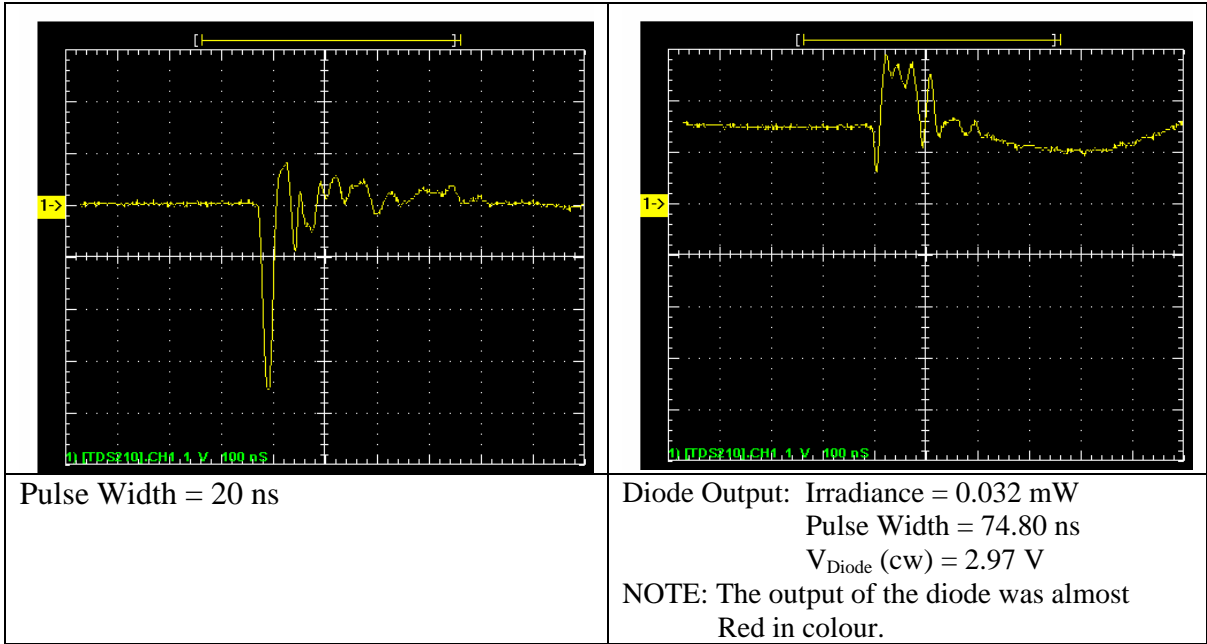
Specifications

Colour	Wavelength (nm)	Luminous Intensity (Typ.) mcd @ If(mA)	Viewing Angle (X2 Theta)
Verde Green	501	9000 350	120 degrees



**Using the Power Measured at Ten Centimeters
From the 475-1199-1-ND LED at Zero Degrees,
This is a Plot of the Distance Required to
Measure the Same Power Level at Angles around
the LED**



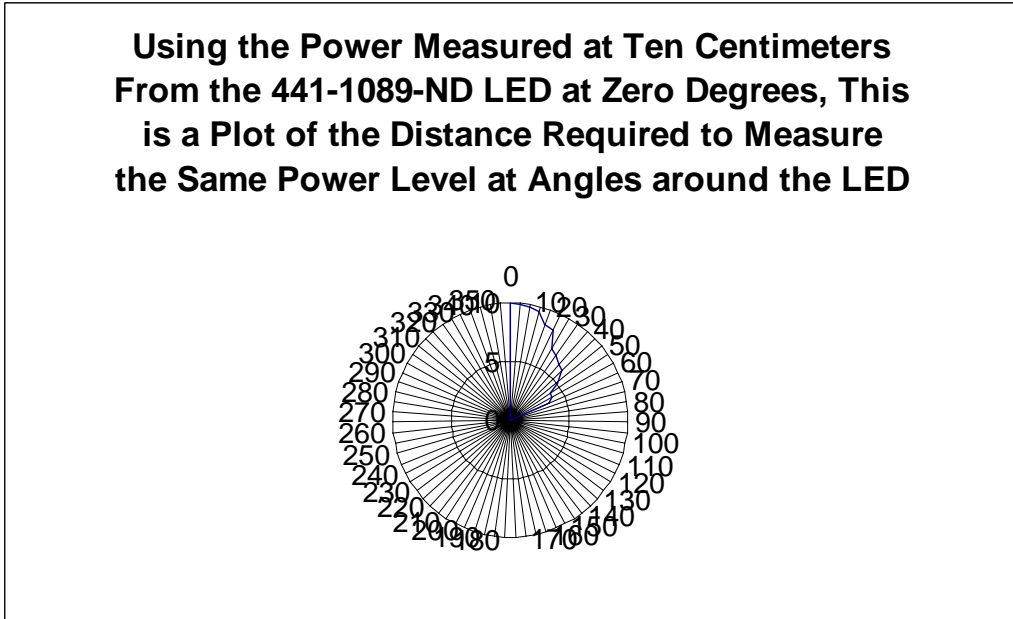
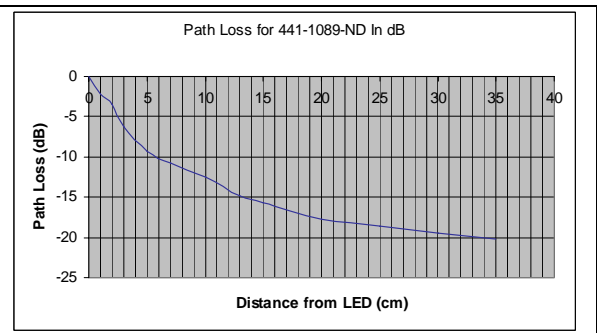
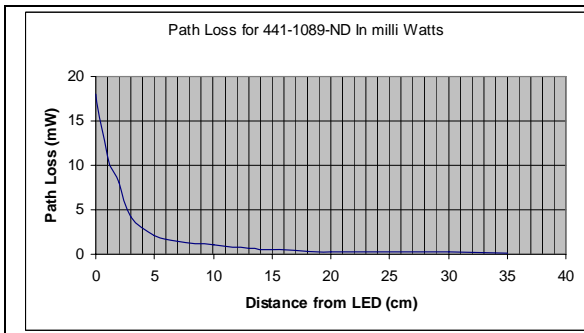
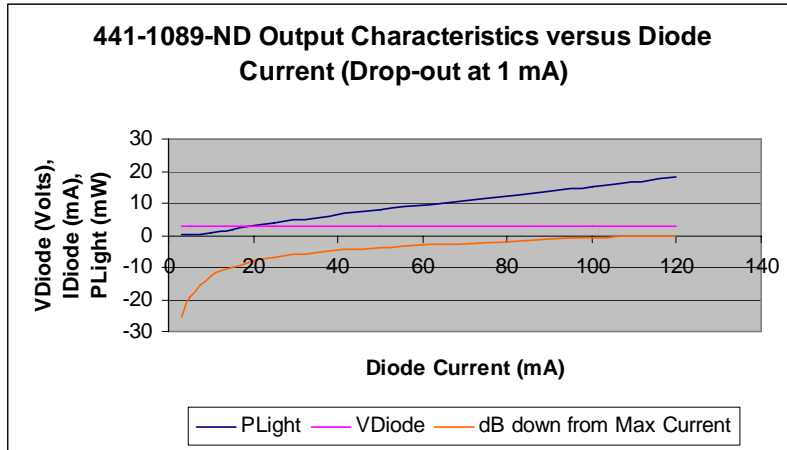


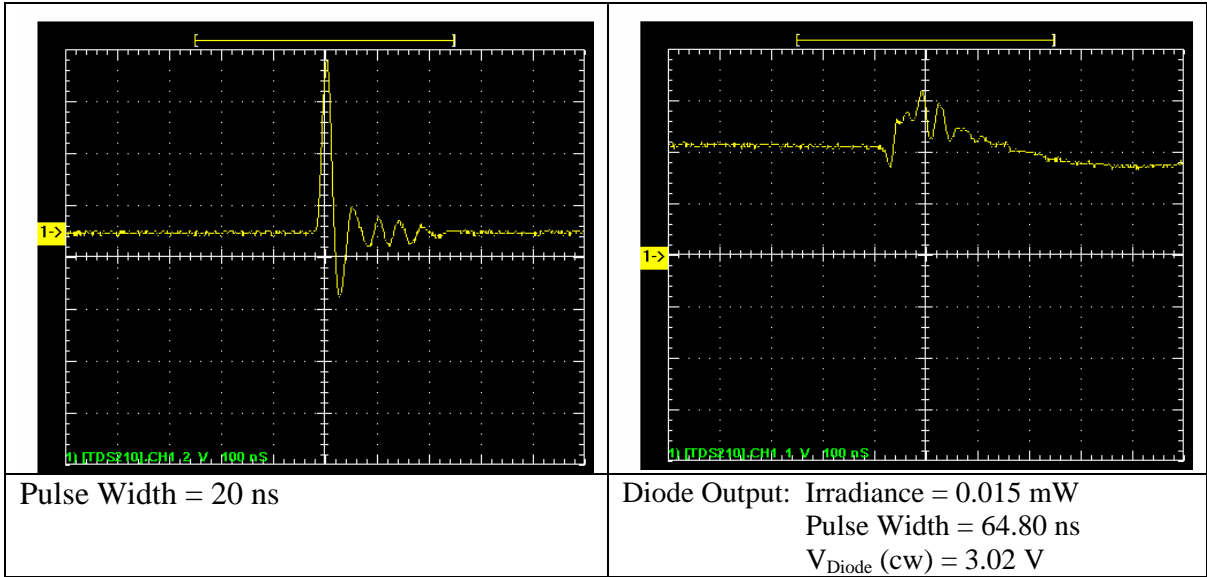
Measurement Method	Automatic	
Measurement	Value	Units
Frequency	11.308M	Hz
Pos. Pulse Width	74.800n	S
Neg. Pulse Width	13.633n	S
Rise Time	11.200n	S
Fall Time	N/A	N/A
Pos. Duty Cycle	845.83m	%
Neg. Duty Cycle	154.17m	%
Pos. Overshoot	0.0000	%
Neg. Overshoot	0.0000	%
Peak to Peak	2.2000	V
Amplitude	2.2000	V
High	2.8800	V
Low	680.00m	V
Maximum	2.8800	V
Minimum	680.00m	V
Mean	1.4531	V
Cycle Mean	2.3209	V
RMS	1.5039	V
BurstWidth	105.80n	S
Period	88.433n	S
Energy	2.2610u	
CEnergy	497.84n	
ACRMS	386.81m	V
CRMS	2.3727	V

4.2.17. 441-1089-ND [13]

Specifications

Colour	Wavelength (nm)	Luminous Intensity (Typ.) mcd @ If(mA)	Viewing Angle (X2 Theta)
Green	525	16000 120	10 degrees



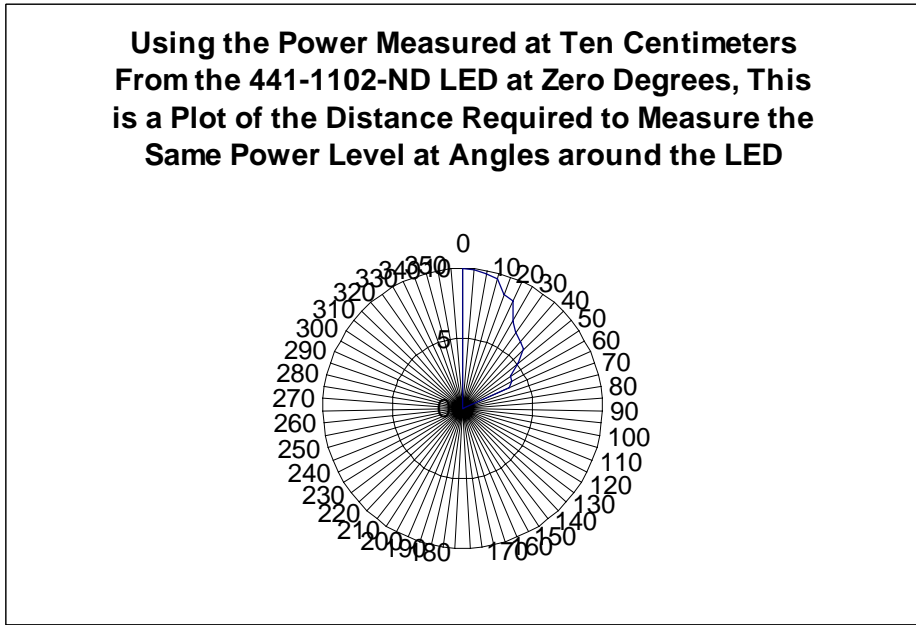
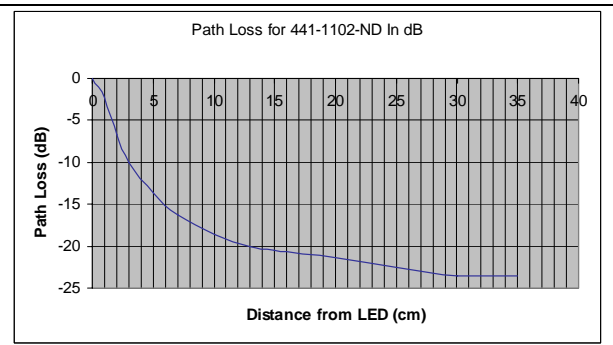
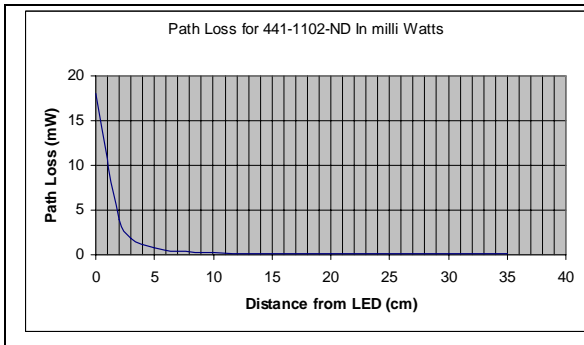
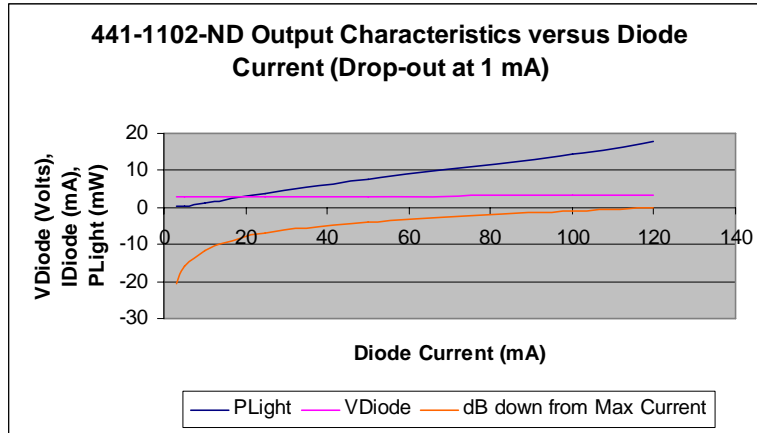


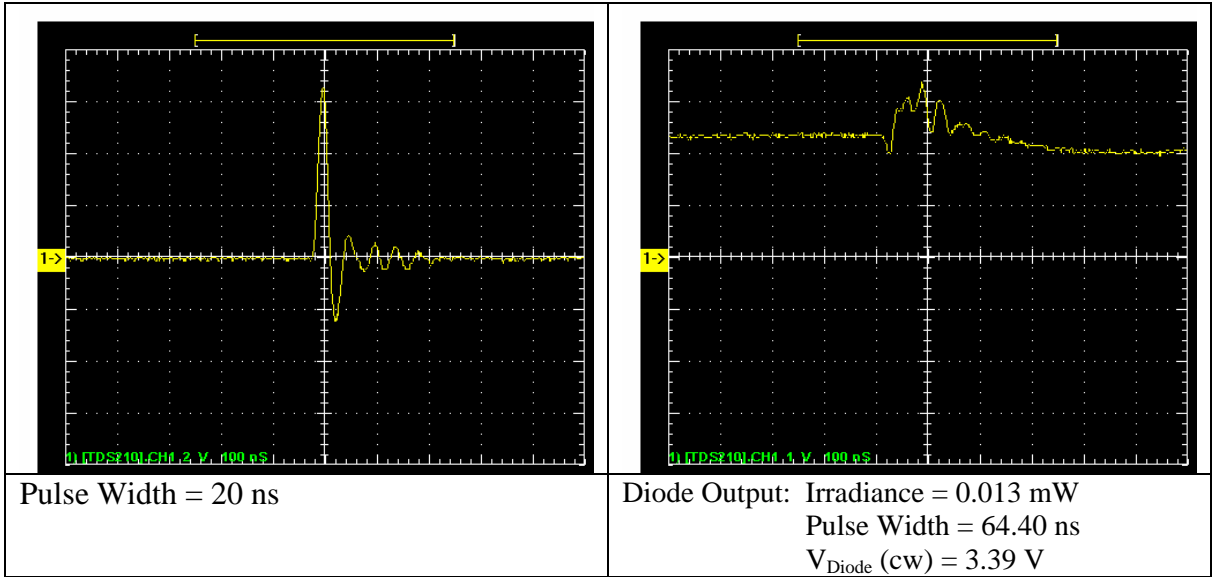
Measurement Method	Automatic	
Measurement	Value	Units
Frequency	13.228M	Hz
Pos. Pulse Width	64.800n	S
Neg. Pulse Width	10.800n	S
Rise Time	53.040n	S
Fall Time	247.04n	S
Pos. Duty Cycle	857.14m	%
Neg. Duty Cycle	142.86m	%
Pos. Overshoot	0.0000	%
Neg. Overshoot	0.0000	%
Peak to Peak	1.4800	V
Amplitude	1.4800	V
High	3.2000	V
Low	1.7200	V
Maximum	3.2000	V
Minimum	1.7200	V
Mean	2.1309	V
Cycle Mean	2.7291	V
RMS	2.1501	V
BurstWidth	141.60n	S
Period	75.600n	S
Energy	4.6210u	
CEnergy	570.39n	
ACRMS	283.50m	V
CRMS	2.7468	V

4.2.18. 441-1102-ND [13]

Specifications

Colour	Wavelength (nm)	Luminous Intensity (Typ.) mcd @ If(mA)	Viewing Angle (X2 Theta)
Blue	470	1600 120	100 degrees



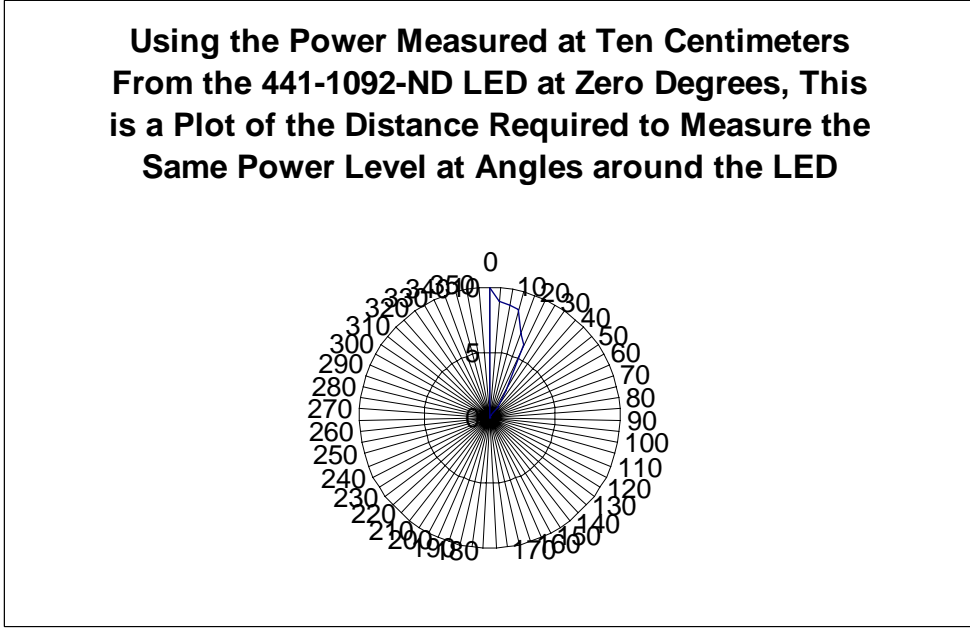
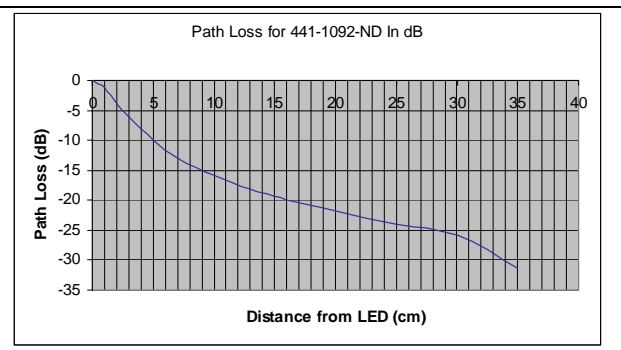
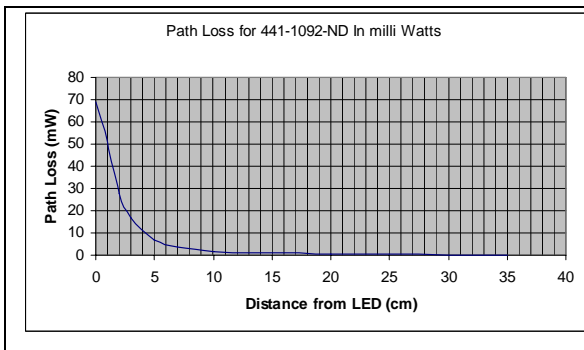
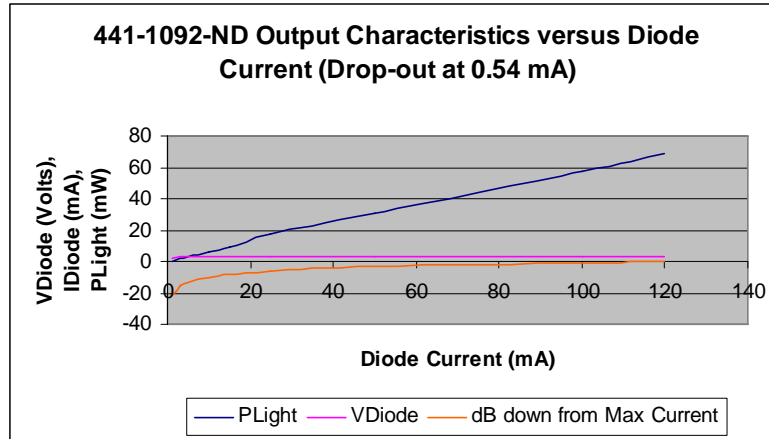


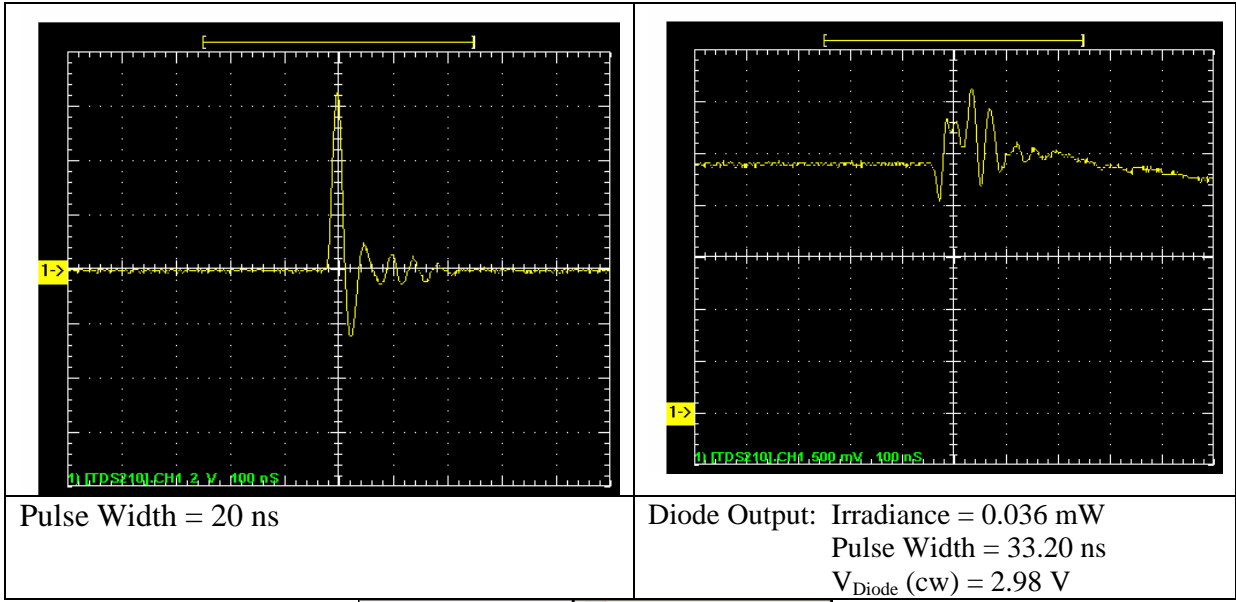
Measurement Method	Automatic	
Measurement	Value	Units
Frequency	13.089M	Hz
Pos. Pulse Width	64.400n	S
Neg. Pulse Width	12.000n	S
Rise Time	55.200n	S
Fall Time	234.40n	S
Pos. Duty Cycle	842.93m	%
Neg. Duty Cycle	157.07m	%
Pos. Overshoot	0.0000	%
Neg. Overshoot	0.0000	%
Peak to Peak	1.4000	V
Amplitude	1.4000	V
High	3.3600	V
Low	1.9600	V
Maximum	3.3600	V
Minimum	1.9600	V
Mean	2.3210	V
Cycle Mean	2.8891	V
RMS	2.3349	V
BurstWidth	99.600n	S
Period	76.400n	S
Energy	5.4493u	
CEnergy	645.27n	
ACRMS	249.65m	V
CRMS	2.9062	V

4.2.19. 441-1092-ND [13]

Specifications

Colour	Wavelength (nm)	Luminous Intensity (Typ.) mcd @ If(mA)	Viewing Angle (X2 Theta)
Blue	470	12,000 120	10 degrees



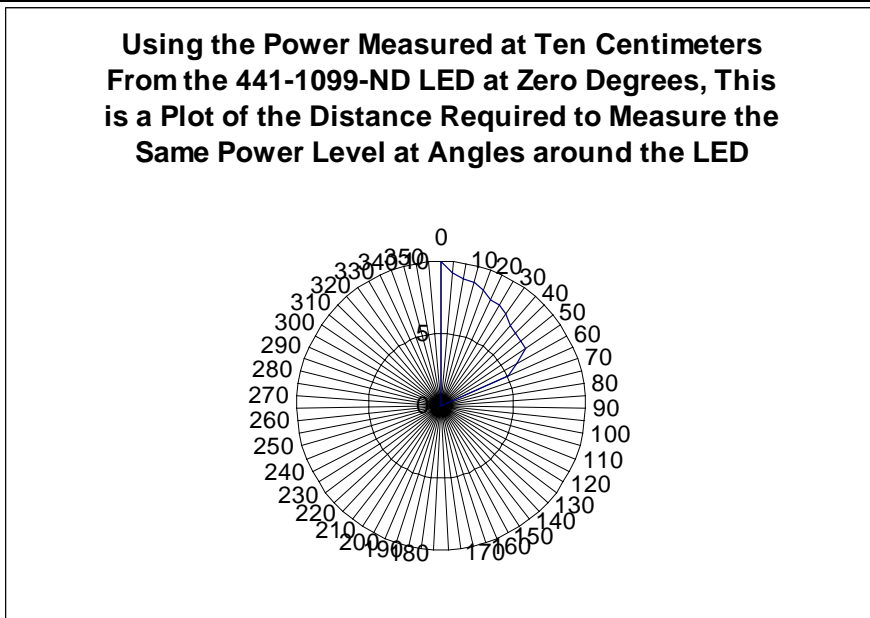
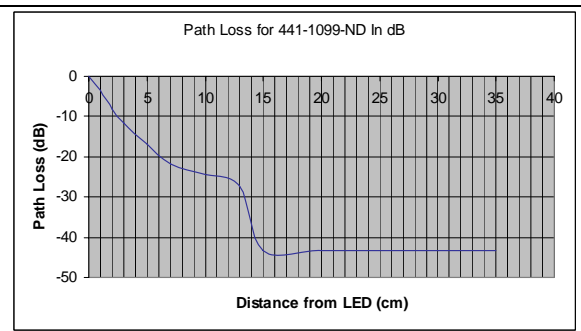
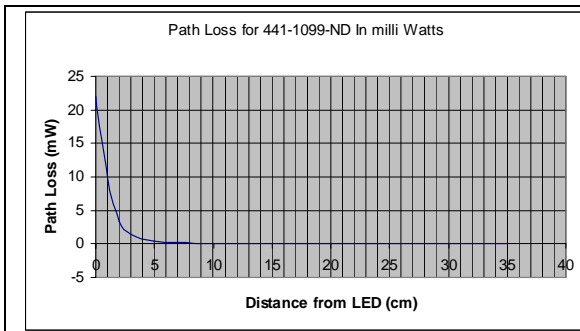
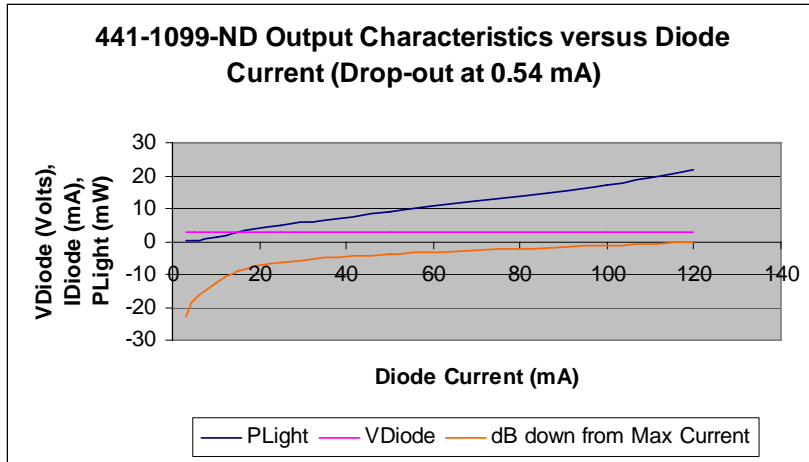


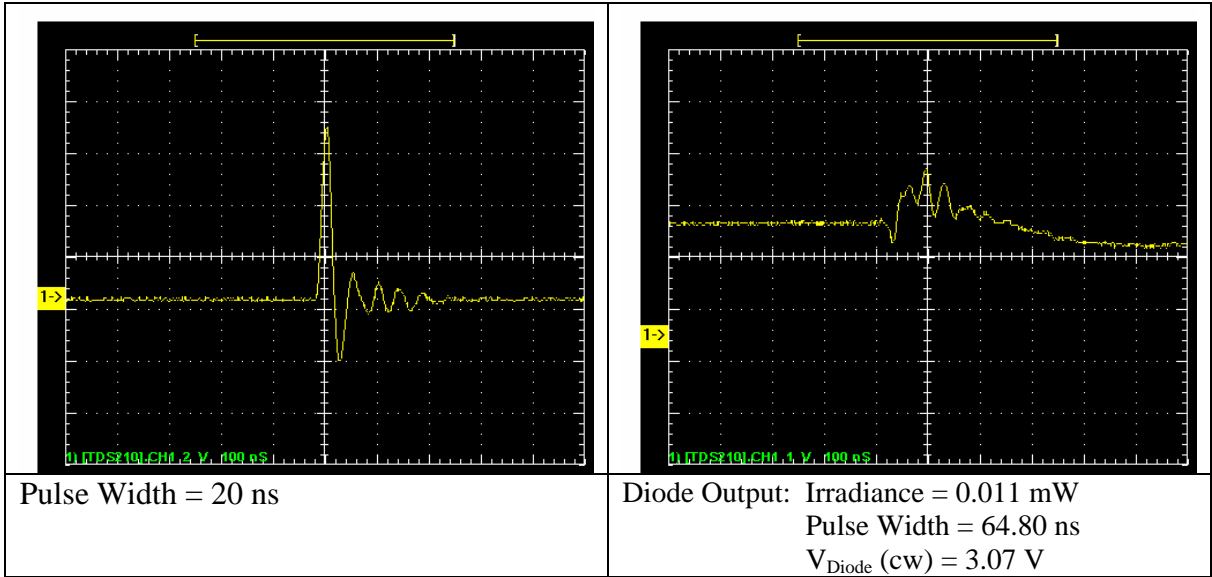
		S210].Data.Waveforms.C	
Measurement Method	Automatic		
Measurement	Value	Units	
Frequency	12.626M	Hz	
Pos. Pulse Width	33.200n	S	
Neg. Pulse Width	46.000n	S	
Rise Time	55.680n	S	
Fall Time	N/A	N/A	
Pos. Duty Cycle	419.19m	%	
Neg. Duty Cycle	580.81m	%	
Pos. Overshoot	0.0000	%	
Neg. Overshoot	0.0000	%	
Peak to Peak	1.0800	V	
Amplitude	1.0800	V	
High	3.1200	V	
Low	2.0400	V	
Maximum	3.1200	V	
Minimum	2.0400	V	
Mean	2.4273	V	
Cycle Mean	2.6874	V	
RMS	2.4316	V	
BurstWidth	143.20n	S	
Period	79.200n	S	
Energy	5.9101u		
CEnergy	579.04n		
ACRMS	135.99m	V	
CRMS	2.7039	V	

4.2.20. 441-1099-ND [13]

Specifications

Colour	Wavelength (nm)	Luminous Intensity (Typ.) mcd @ If(mA)	Viewing Angle (X2 Theta)
Green	525	1600 120	100 degrees





Measurement Method	Automatic	
Measurement	Value	Units
Frequency	8.5324M	Hz
Pos. Pulse Width	64.800n	S
Neg. Pulse Width	52.400n	S
Rise Time	57.360n	S
Fall Time	263.36n	S
Pos. Duty Cycle	552.90m	%
Neg. Duty Cycle	447.10m	%
Pos. Overshoot	0.0000	%
Neg. Overshoot	0.0000	%
Peak to Peak	1.5200	V
Amplitude	1.5200	V
High	3.2000	V
Low	1.6800	V
Maximum	3.2000	V
Minimum	1.6800	V
Mean	2.1274	V
Cycle Mean	2.6845	V
RMS	2.1474	V
BurstWidth	144.00n	S
Period	117.20n	S
Energy	4.6096u	
CEnergy	854.42n	
ACRMS	289.10m	V
CRMS	2.7001	V

4.3. Performance Analysis

The most important performance specification for sensor networks is power conservation. The measure of input current versus irradiant power is the measure of the LED's use of energy. The diode with part number RL5-B4630 exhibited the highest irradiant power (15 mW) at maximum current of 20 mA. The diode with part number 475-1198-1-ND has a rated maximum current of 350 mA (at which current the irradiant power was 113 mW). This would appear to be a problem with respect to power conservation, however, with its input current reduced to 20 mA, the irradiant power is still 15 mW (the same as for RL5-B4630). 475-1198-1-ND has an advantage over RL5-B4630 in that its viewing angle is much wider (120° as compared to 30°) so this diode, in fact, provides superior characteristics for both power conservation and viewing angle. The wavelength of 475-1198-1-ND is 465 nm (blue light) which has an attenuation coefficient of approximately 0.75 m^{-1} in turbulent coastal waters (see Figure 7). This is close to the stated best attenuation coefficient $K(490)$.

Path loss was higher than expected for all diodes. In many cases a 3 dB (half power) drop occurred in the first centimetre. Also in all cases irradiance had dropped to a level near ambient conditions at 35 cm making measurements very difficult beyond this range. These measurements were made in air. It is expected that in water, in particular in turbid sea water, that path loss would be even greater. The percent of irradiated power values in Table 1 could be used as a correction factor to predict an even greater loss. CSAIL [15] has deployed an undersea optical sensor network that claims a 320 kbps transmission rate optical communication over a maximum 2.2 m range.

The minimum pulse width measured from the diodes was approximately 80 ns for the low current diodes. The higher current diodes (including 475-1198-1-ND) operated to pulse widths as low as 20 ns. The minimum pulse width may have been even smaller for the high current diodes, however loading effects and limitations of the driving circuits seemed to interfere with the measurements.

5. Conclusions

Light emitting diodes working in the visible spectrum between violet and green may be used as transmitters for an undersea optical sensor network. These diodes must penetrate the water over a suitable distance in order to communicate with other sensor nodes. The diodes tested in this project were able to penetrate air over a range of approximately 35 cm. This distance is unlikely to be sufficient. A further search for light emitting diodes capable of longer range communication is warranted.

The important criterion of power conservation was investigated. Although the lower current diodes would appear to be the best choice in order to conserve power, in fact the higher current diodes used at lower power levels outperformed the low

current diodes. These high current diodes had wider viewing angles, better penetration and could be operated at narrower pulse widths.

6. Recommendations

The following are recommendations for further research:

- Detection devices and detection circuits need to be investigated. Detection devices such as PIN diodes, Avalanche Photo Detection diodes (APD's) and LED's may be suitable as detection devices.
- Transmitting high intensity light from the sea bed may have environmental implications. Such light may be hazardous to under sea life including fish, reefs or even divers. An environmental impact study would help to determine what, if any, negative impact may result from deployment of such a sensor network.
- It would be valuable to determine if fading is an issue. The effects of reflection, diffraction, refraction and scattering should be measured. In addition, an investigation of acoustic effects on optical transmission should be undertaken.
- A suitable MAC layer protocol needs to be determined. This should be an energy conservation protocol. Such protocols currently exist. It is important to investigate these protocol in order to determine if an appropriate protocol currently exist or if a new protocol needs to be developed for this application.

7. References

- [1] VENUS Home, <http://www.venus.uvic.ca/index.html>
- [2] Information for Backgrounder on Venus Release, <http://www.venus.uvic.ca/documents/Background-on-VENUS.pdf>
- [3] Wikipedia, <http://en.wikipedia.org/wiki>
- [4] IEEE Communications Magazine, August 2002, <http://w5.cs.uni-sb.de/teaching/ss06/IE/Literatur/SurveySensorNets.pdf>
- [5] Light Absorption & Scattering in Water Samples, D & A Instrument Company, http://www.d-a-instruments.com/light_absorption.html
- [6] Physical properties of seawater, http://ccar.colorado.edu/asen5215/chapter_3_120604.doc
- [7] Ackleson, Steve G., "Diffuse attenuation in optically-shallow water: effects of bottom reflectance", Office of Naval research, Arlington, Va., SPIE Vol. 2963.
- [8] Kishino, M., Ishizaka, J., Datoh, H., Kusaka, K., Saitoh, S., Miyoi, T., Kawasaki, K., "Optical characteristics of seawater in the North Pacific Ocean, Japan, SPIE Vol. 2963.
- [9] Stallings, William, "Data and Computer Communications, 7th edition", Pearson Education Inc., Toronto, 2004.
- [10] Shankar, Mohana P., "Introduction to Wireless Systems", John Wiley and Sons, New york, 2002.
- [11] Atmospheric Turbulence in Free-Space Optical Communication, <http://www-ee.stanford.edu/~jmk/research/turb.html>
- [12] Acousto-Optic Effect, http://acoustooptics.phys.msu.ru/ao_effect.asp

- [13] Digikey Online Catalog, <http://dkc3.digikey.com/PDF/C062/DigiKey.pdf>
- [14] Super Bright LED's Inc., <http://www.superbrightleds.com/leds.htm>
- [15] Optical and Acoustical Underwater Sensor Network,
<http://publications.csail.mit.edu/abstracts/abstracts05/rus6/rus6.html>

Appendix A. Light Emitting Diodes Investigated

DigiKey		www.ca.digikey.com				
Part Number	Colour	Wavelength (mm)	Vf(V) typ	If(mA) max	Io(mcd)	Viewing Angle (2xTheta)
67-1115-ND	Sup. Yellow	590	2.1	30	1000	30
67-1755-ND	Green	502	3.5	25	1500	30
Part Number	Colour	Wavelength (mm)	Vf(V) min	LED Current (@1.5V)	Typ mcd @ 2V	Viewing Angle (2xTheta)
SSL-DSP5093UPGC Lumex Part No.	Green	525	1.5	2.5	3500	30
SSL-DSP5093USBC Lumex Part No.	Blue	470	1.5	2.5	2500	30
Part Number	Colour	Wavelength (mm)	Vf(V) typ	If (mA) max	Io (mcd)	Viewing Angle (2xTheta)
441-1089-ND	Green	525	3.4	120	16,000	10
441-1092-ND	Blue	470	3.4	120	12,000	10
441-1099-ND	Green	525	3.4	120	1600	100
441-1102-ND	Blue	470	3.4	120	1600	100
Part Number	Colour	Wavelength (mm)	Vf(V)	If (mA)	Typ. mcd @ Current (mA)	Viewing Angle (2xTheta)
475-1126-1-ND	True Green	520	3.8	500	10,000 350	120
475-1198-1-ND	Blue	465	3.8	500	2700 350	120
475-1199-1-ND	Verde Green	501	3.8	500	9000 350	120
Part Number	Colour	Wavelength (mm)			Luminous Intensity (Typ.) mcd @If(mA)	Viewing Angle (2xTheta)
OVLFB3C7 TT Electronics Part No.	Blue	470			1350 20	30
OVLFG3C7 TT Electronics Part No.	Green	525			5200 20	30
OVLGCOC6B9 TT Electronics Part No.	Blue-Green	505			8000 20	6

Superbright LEDs Inc		www.superbrightleds.com			
Part Number	Colour	Luminous Intensity (mcd)	Viewing Angle	Wave Length (nm)	
RL5-B4630	Blue	4600	30	472	
RL5-B5515	Blue	5500	15	470	
RL5-G8045	Green	8000	45	525	
RL5-G7532	Green	7500	32	525	
RL5-A7032	Aqua	7000	32	507	
RL5-V1015	Violet	1000	15	420	

Appendix B. Circuit Designs

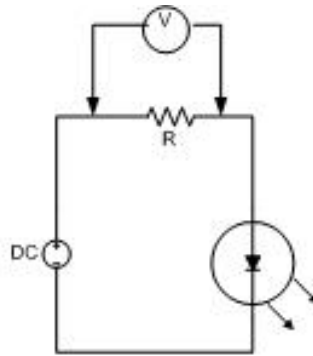


Figure 16
Unbuffered LED Circuit

For the circuit in Figure 16: $R = \frac{V_{DC}}{I_{Diode}}$

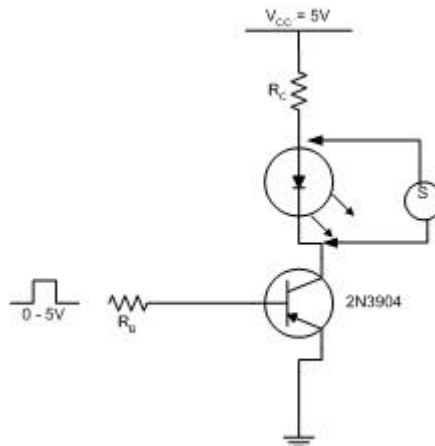


Figure 17
Buffered LED Circuit

For the buffered diode driver circuit shown in Figure 17:

$$R_C = \frac{V_{CC} - V_{Diode} - V_{CE(SAT)}}{I_{Diode}} \quad \text{Use } V_{CE(SAT)} = 0.3V$$

$$I_B = \frac{I_{Diode}}{\beta_{SAT}} \quad \text{Use } \beta_{SAT} = 50$$

$$R_B = \frac{V_{IN} - V_{BE}}{I_B} \quad \text{Use } V_{BE} = 0.7V, V_{IN} = 5V$$